

**SYNTHESIS AND CHARACTERIZATION OF CARBON
NANOMATERIALS USING
BIS(ACETYLACETONATO)OXOVANADIUM(IV), MANGANESE(III)
ACETYLACETONATE, Co-Zn and Co-Al AS CATALYST
PRECURSORS**

**Silindile Nomathemba Ndwandwe
MASTER OF TECHNOLOGY THESIS**

VAAL UNIVERSITY OF TECHNOLOGY

2011

**SYNTHESIS AND CHARACTERIZATION OF CARBON NANOMATERIALS USING
BIS(ACETYLACETONATO)OXOVANADIUM(IV), MANGANESE(III)
ACETYLACETONATE, Co-Zn and Co-Al AS CATALYST PRECURSORS**

By

Silindile Nomathemba Ndwandwe

Submitted in fulfilment of the requirements for the degree

MASTER OF TECHNOLOGY

In

Chemistry

Supervisor: Prof. E. D. Dikio

Date submitted

July 2011

DECLARATION

I hereby declare that this dissertation, which am submitting for the qualification of

Masters of Technology in Chemistry

To the Vaal University of Technology, Faculty of Applied and Computer Science, Department of Analytical Chemistry, is apart from the recognized supervisor and the sources that have been acknowledged in literature survey, entirely my own work and has not previously been submitted to any other institution before for a research diploma or degree.

Signature of a candidate

date

Signature of a supervisor

date

DEDICATION

I dedicate this work to the Ndwandwe and Qwabe family especially my mother Dingeni Qwabe Ndwandwe, sisters Sne, Dudu, Sanele, Pamela, Sandisiwe and my late grandmother Hambezandisa Magwaza Qwabe. I thank you all for all the support, inspiration and motivation you gave me.

ACKNOWLEDGEMENTS

I would like acknowledge the following people and organizations for their valuable contribution and assistance in the execution of this research project

- Dr E. D. Dikio, my supervisor for the help and guidance throughout this dissertation.
- Edward Nxumalo of University of Witwatersrand, School of Chemistry, for assisting with the TGA analysis.
- The Vaal University of Technology in collaboration with the National Research Foundation (NRF) and SASOL for financial support.
- CSIR for assisting with the Raman, EDS, XRD, SEM and TEM analysis.
- Special thanks to my parents, siblings and friends for their support during the period of my study.
- Finally, I would love to thank the Almighty who has been with me through out and provided me with the strength to carry out this study to finish.

ABSTRACT

Bis(acetylacetonato)oxovanadium(IV), Manganese(III) acetylacetonate, Co-Zn and Co-Al were prepared as catalyst precursors for the synthesis of carbon materials in a catalytic chemical vapor deposition (CCVD) reactor. The carbon materials produced were characterized with Raman spectroscopy, Scanning electron microscope (SEM), Energy dispersive spectroscopy (EDS), X-ray diffraction (XRD), High resolution transmission electron microscopy (TEM) and Thermogravimetric analysis, (TGA).

Carbon material prepared from bis(acetylacetonato)oxovanadium(IV) catalyst precursor showed the presence of carbon spheres with average diameter of 104 μ m together with small traces of carbon nanotubes or amorphous carbon. Synthesis of bis(acetylacetonato)oxovanadium(IV) catalyst precursor yielded approximately 92% of carbon material. Carbon material prepared from Manganese(III) acetylacetonate catalyst precursor showed the presence of carbon spheres with diameter of 87.5 μ m. Synthesis of Manganese(III) acetylacetonate catalyst precursor yielded approximately 97% of carbon material.

Carbon material produced from Co-Zn and Co-Al catalyst precursors showed the presence of carbon nanotubes with small amounts of amorphous carbon. The use of Co-Zn catalyst precursor yielded approximately 80% of carbon nanotubes, whereas Co-Al catalyst precursor yielded approximately 98% of carbon nanotubes.

TABLE OF CONTENTS

Description	Page number
Declaration	i
Dedication	ii
Acknowledgements	iii
Abstract	iv
Table of contents	v
List of figures	ix
List of equations	xi
List of abbreviations	xii

CHAPTER ONE

INTRODUCTION

1.1 Background	1
1.2 Objectives	2
1.3 Outline of the dissertation	3
References	5

CHAPTER TWO

LITERATURE REVIEW

2.1 Introduction	6
2.2 Organometallic compounds	6
2.2.1 Acetylacetonate	7

Description	Page number
--------------------	--------------------

2.3 Carbon nanomaterials	10
2.3.1 Carbon nanotubes	11
2.3.1.1 Single-walled carbon nanotubes	13
2.3.1.2 Multi-walled carbon nanotubes	14
2.3.2 Carbon nanospheres	15
2.4 Synthesis methods	16
2.4.1 Catalytic chemical vapor disposition	16
2.4.2 Arc-discharge method	20
2.4.3 Laser ablation method	20
2.4.4 Nebulizer spray pyrolysis	21
References	22

CHAPTER THREE

EXPERIMENTAL METHODS

3.1 Introduction	28
3.2 Chemicals and materials	28
3.3 Preparation of the precursors	28
3.3.1 Bis(acetylacetonato)oxovanadium(IV)	28
3.3.2 Manganese(III) acetylacetonate	29
3.3.3 Co-Zn and Co-Al	30
3.4 Characterization of the precursor	30

Description

Page number

3.5 Production of carbon nanomaterials	31
3.6 Characterization of carbon nanomaterials	32
3.6.1 Raman spectroscopy	32
3.6.2 Scanning electron microscopy	33
3.6.3 Energy dispersive spectroscopy	34
3.6.4 X-ray diffraction	34
3.6.5 Transmission electron microscopy	34
3.6.6 Thermogravimetric analysis	35
References	36

CHAPTER FOUR

RESULTS AND DISCUSSION

4.1 Introduction	38
4.2 Characterization of the catalyst precursors	38
4.3 Characterization of carbon nanomaterials	44
4.3.1 Carbon nanomaterials as-prepared from bis(acetylacetonato)oxovanadium(IV)	44
4.3.2 Carbon nanomaterial as-prepared from Manganese(III) acetylacetonate	53
4.3.3 Carbon nanomaterial as-prepared from Co-Zn	58
4.3.4 Carbon nanomaterial as-prepared from Co-Al	63

Description

Page number

CHAPTER FIVE

CONCLUSION

68

RECOMMENDATIONS

69

References

70

LIST OF FIGURES

Page number

2.1 Keto- and enol- form	7
2.2 Diketone derivates	9
2.3 Bis(acetylacetonato)oxovanadium(IV)	10
2.4 SWCNT`s with singular grapheme cylindrical walls	13
2.5 MWCNT`s with multi layers of grapheme cylindrical walls	15
3.1 Schematic diagram of the CCVD process	32
4.1 FTIR spectra of pure acetylacetonate	41
4.2 FTIR spectra of bis(acetylacetonato)oxovanadium(IV)	42
4.3 FTIR spectra of Manganese(III) acetylacetonate	43
4.4 Raman spectra of carbon materials as-prepared from bis(acetylacetonato)oxovanadium(IV)	45
4.5 SEM images of carbon material as-prepared from bis(acetylacetonato)oxovanadium(IV)	46
4.6 EDS spectrum of carbon material as-prepared from bis(acetylacetonato)oxovanadium(IV)	47
4.7 XRD pattern of carbon material as-prepared from bis(acetylacetonato)oxovanadium(IV)	49
4.8(a) TEM micrograph of carbon material as-prepared from bis(acetylacetonato)oxovanadium(IV)	50
4.8(b) TEM micrograph of carbon material as-prepared from bis(acetylacetonato)oxovanadium(IV)	51
4.9 TGA data of carbon material as-prepared from bis(acetylacetonato)oxovanadium(IV)	52
4.10 Raman spectrum of carbon material as-prepared from Manganese(III) acetylacetonate	53

4.11 XRD pattern of carbon material as-prepared from Manganese(III) acetylacetonate	54
4.12(a) TEM micrograph of carbon material as-prepared from Manganese(III) acetylacetonate	55
4.12(b) TEM micrograph of carbon material as-prepared from Manganese(III) acetylacetonate	56
4.13 TGA data of carbon material as-prepared from Manganese(III) acetylacetonate	57
4.14 Raman spectrum of carbon nanomaterial as-prepared from Co-Zn	59
4.15 SEM image of carbon nanomaterial as-prepared from Co-Zn	60
4.16 EDS spectrum of carbon nanomaterial as-prepared from Co-Zn	61
4.17 XRD pattern of carbon nanomaterial as-prepared from Co-Zn	62
4.18 Raman spectrum of carbon nanomaterial as-prepared from Co-Al	64
4.19 SEM image of carbon nanomaterial as-prepared from Co-Al	65
4.20 EDS spectrum of carbon nanomaterial as-prepared from Co-Al	66
4.21 XRD pattern of carbon nanomaterial as-prepared from Co-Al	67

LIST OF EQUATIONS

- 1) bis(acetylacetonato)oxovanadium(IV)
- 2) Manganese(III) acetylacetonate

LIST OF ABBREVIATIONS AND ACRONYMS

Min	-	Minutes
CNT`s	-	Carbon nanotubes
CNS`s	-	Carbon nanospheres
SWCNT`s	-	Single-walled carbon nanotubes
MWCNT`s	-	Multi-walled carbon nanotubes
CCVD	-	Catalytic chemical vapour deposition
VO(acac) ₂	-	Bis(acetylacetonato)oxovanadium(IV)
Mn(acac) ₃	-	Manganese(III) acetylacetonate
C1	-	Carbon one
Zn	-	Zinc
Co	-	Cobalt
Al	-	Aluminium
M-C	-	Metal carbon
FTIR	-	Fourier Transform Infrared
SEM	-	Scanning electron microscopy
EDS	-	Energy dispersive spectroscopy
XRD	-	X-ray diffraction
TEM	-	Transmission electron microscopy
TGA	-	Thermogravimetric analysis

1.1 BACKGROUND

Carbon nanomaterials have attracted enormous attention because of their unique structure, low density, high porosity, large surface area, high chemical and thermal stability and their ability to store large amount of hydrogen.¹⁻⁴ There are a number of carbon nanostructures that have been discovered over the past years such as carbon nanotubes (CNT`s), nanofibers, nano-anions, nanocapsules, and carbon nanospheres (CNS`s) that results from the carbon`s ability to hybridize sp , sp^2 and sp^3 bonds.⁴ The commonly researched carbon nanostructures are CNT`s and CNS`s.⁵

CNS`s results from the sp^2 hybridization of carbon bond. These nanomaterial differ from other carbon nanomaterials in their nanostructure, they have a spherical structure or enclosed graphene layers whereas CNT`s, nano-anions and nanocapsule have a tubular like structure that is open on each end.⁶ CNT`s are a new form of carbon that was discovered in 1991.⁷ Having a concentric graphitic cylinders closed at either end due to the presence of five-membered rings with the carbon atoms tiling on a spherical or nearly spherical surfaces⁸ and a very small particle size that is measured in nanometers.⁹

CNT`s possess some very unique characteristics due to their hollow center, nanometer size, large surface area and the ability to change their electrical resistance drastically when exposed to alkalines, halogens and other gases at room temperature.¹⁰ The honeycomb-shaped walls of CNT`s consist of either a single layer of carbon atoms known as a single-walled carbon nanotubes (SWCNT`s) or multiple layers of carbon atoms known as multi-walled carbon nanotubes (MWCNT`s).⁸ SWCNT`s are considered as a sheet of graphene that has been rolled up into a

seamless cylinder with a singular graphene cylindrical wall.¹⁰ With a high ability to predict properties of nanotubes based on their theoretical structure and are relatively simple compare to the MWCNT`s.¹¹

MWCNT`s are considered as sheets of graphene that had been rolled up into a seamless cylinder with multi graphene cylindrical wall. MWCNT`s have a central tube of nanometric diameter surrounded by graphitic layers separated by ~0.34 nm with a well defined shape, composition, high aspect ratio, mechanically robust, excellent wear properties and chemical fictionalization at the tip.¹⁰

There are three methods that are a major synthesis routes for the production of carbon nanomaterials.⁹⁻¹⁰ These methods are laser arc discharge, laser ablation and catalytic chemical vapor deposition.¹¹⁻¹³

1.2 OBJECTIVES

The objective of this study is:

- To synthesize bis(acetylacetonato)oxovanadium(IV) and Manganese(III) acetylacetonate as catalyst precursors to produce carbon nanomaterials.
- To synthesize Cobalt-Zinc and Cobalt-Aluminium as catalyst precursors to produce carbon nanomaterials.
- To study the characteristics of the produced carbon nanomaterials using different analytical techniques.

- To determine the nanostructures of the synthesized bis(acetylacetonato)oxovanadium(IV), Manganese(III) acetylacetonate, Cobalt-Zinc and Cobalt-Aluminium catalyst precursors.

1.3 OUTLINE OF THE DISSERTATION

Below is an outline of this dissertation

Chapter 1 (Introduction): This chapter gives insight on the research work that was carried out and its importance. Also presented in this chapter are the problem statement and the objectives of this study.

Chapter 2 (Background study): In this chapter, a review of literature pertaining to organometallic compounds and carbon nanomaterials, and their carbon nanostructures.

Chapter 3 (Methodology): All analytical methods, experimental procedures and instruments that were used in this research project are discussed in details in this chapter.

Chapter 4 (Results and discussion): Results obtained from this study are presented and discussed in chapter 4.

Chapter 5 (Conclusion and recommendation): Based on the results obtained with respect to the initial objectives and hypothesis, conclusions are drawn and

highlighted in this last chapter. Recommendations for future work are presented in chapter 5.

REFERENCES

1. H. Dai, *Surf. Sci.* 500 (2002) 218-241.

2. M.S. Dresselhaus, Y.M. Lin, O. Rabin, A. Jorio, A.G. Souza Filho, M.A. Piment, R. Saito Ge, G. Samsonidze, G. Dresselhaus, *Mat. Sci. Eng.* 23 (2003) 129-140.
3. H. Yang, S.C. Wang, D.L. Akins, *Chem. Phys. Lett.* 416 (2005) 18-21.
4. R.R. He, H.Z. Jin, Y.J. Yan, X.H. Chen, *Chem. Phys. Lett.* 298 (2) (1998) 170-176.
5. X. Peng, Z. Luan, J. Dng, Z. Di, Y. Li, B. Tian, *Mat. Lett.* 59 (2005) 399.
6. R.E.I. Schropp, B. Stannowski, A.M. Brockhoff, P.A.T.T. Van Veenendaal, J.K. Rath, *Mater. Phys. Mech.* 1(2000) 73-82.
7. S. Iijima, *Nature.* 354(7) (1991) 56-58.
8. L.T. Chadderton, Y. Chen, *Phys. Lett. A.* 263 (4) (1999) 401 - 405.
9. Y.T. Jang, S.I. Moon, J.H. Ahn, Y.H. Lee, B.K. Ju, *Sens. Act. B.* 99 (2004) 118-122.
10. J. Kong, A.M. Cassell, H. Dai, *Chem. Phys. Lett.* 292 (6) (1998) 567-574.
11. J. Bernholc, C. Roland, B.I. Yakobson, *Nano.* 2 (6) (1997) 706-715.
12. S. Karthikeyan, P. Mahalingam, M. Karthik, *J. Chem.* 6 (1) (2009) 1-12.
13. F. Kokai, A. Koshio, M. Shiraishi, T. Matsuta, S. Shimoda, M. Ishihara, Y. Koga, H. Deno, *Diam. Relat. Mat.* 14 (3) (2005) 724-728.

2.1 INTRODUCTION

This chapter focuses on the literature associated with carbon nanomaterials and carbon nanostructures. The catalysts and precursors formed from organometallic compounds is also discussed. This chapter concludes with a review of carbon nanomaterials and carbon nanostructures which form the core of this study.

2.2 ORGANOMETALLIC COMPOUNDS

Organometallic catalysts have attracted a considerable interest over the past few years because of their high and versatility in synthetic chemistry.¹⁻² Organometallic compounds provide a source of nucleophilic carbon atoms which can react with electrophonic carbon to form a new carbon – carbon bond. Organometallics are usually kept in a solution of organic solvents due to their very high reactivity especially when reacting with H₂O and O₂.³

Many complexes feature co-ordination bonds between a metal and organic ligand. The organic ligands often bind the metal through hetero-atoms such as oxygen or nitrogen, such compounds are considered coordination compounds.⁴ However, if any of the ligands form a direct metal-carbon (M-C) bond, then the complex is usually considered to be organometallic, e.g. [(C₆H₆)Ru(H₂O)₃]²⁺.⁵

The M-C bond in organometallic compounds are generally of a character intermediate between ionic and covalent.⁶⁻⁷ Primary ionic M-C bonds are encountered when the metal is very electropositive or when the carbon containing ligand exists as a stable carbanion. Carbanions can be stabilized by resonance or by the presence of electron withdrawing substituents.⁸ The ionic character of M-C bonds

in the organometallic compounds of transition metals, poor metals and metalloids tends to be intermediate, owing to the middle of the road electro-negativity of such metals.⁹ Organometallic compounds with bonds that have characters in between ionic and covalent are very important in industry, as they are both relatively stable in solutions and relatively ionic to undergo reactions.¹⁰

Organometallics find practical use in stoichiometric and catalytic processes, especially processes involving carbon monoxide and alkene derived polymers. All the world's polyethylene and polypropylene are produced via organometallic catalysts, usually heterogeneously via Ziegler-Natta catalysis.¹¹⁻¹²

2.2.1 Acetylacetonate

Acetylacetonate also known as 2,4-pentanedione with a molecular formula $C_5H_8O_2$ is a primary example of organometallic compounds, when reacted with a metal to form an organometallic compound.¹³ Acetylacetonate is a diketone, it has both the keto-form $[CH_3COCH_2COCH_3]$ and enol-form $[CH_3COCH=C(OH)CH_3]$ both coexist in the solution (**as shown in Figure 2.1**). Acetylacetonate is mostly used as a precursor for synthesis of heterocyclic compound.¹⁴

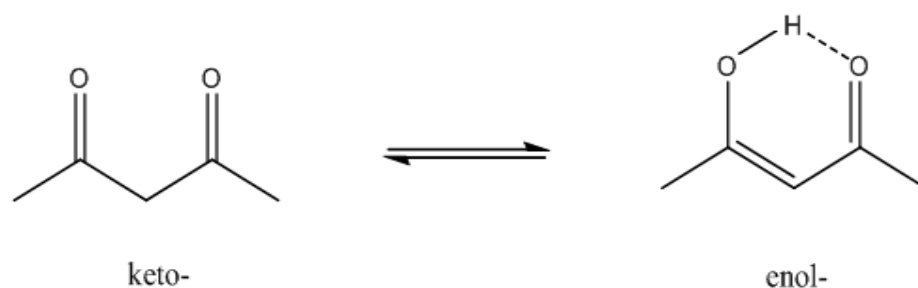


Figure 2.1: *keto- and enol- form*

The keto-enol tautomerism (**as presented in Figure 2.2**) results in the tautomeric migration of hydrogen atom from an adjacent carbon atom to a carbonyl group of keto compound to produce the enol form of the compound.¹⁵ Diketone derivatives are used for several versatile applications and undergo several reversible and irreversible reactions to fulfill the applications that are used for,¹⁶ those reactions are:

- Aldol reactions
- Alkylation of enolate anions
- Clemmensen reduction
- Hemiacetal and acetal formation
- Hydration formation
- Imine formation
- Wolff-Kishner reduction

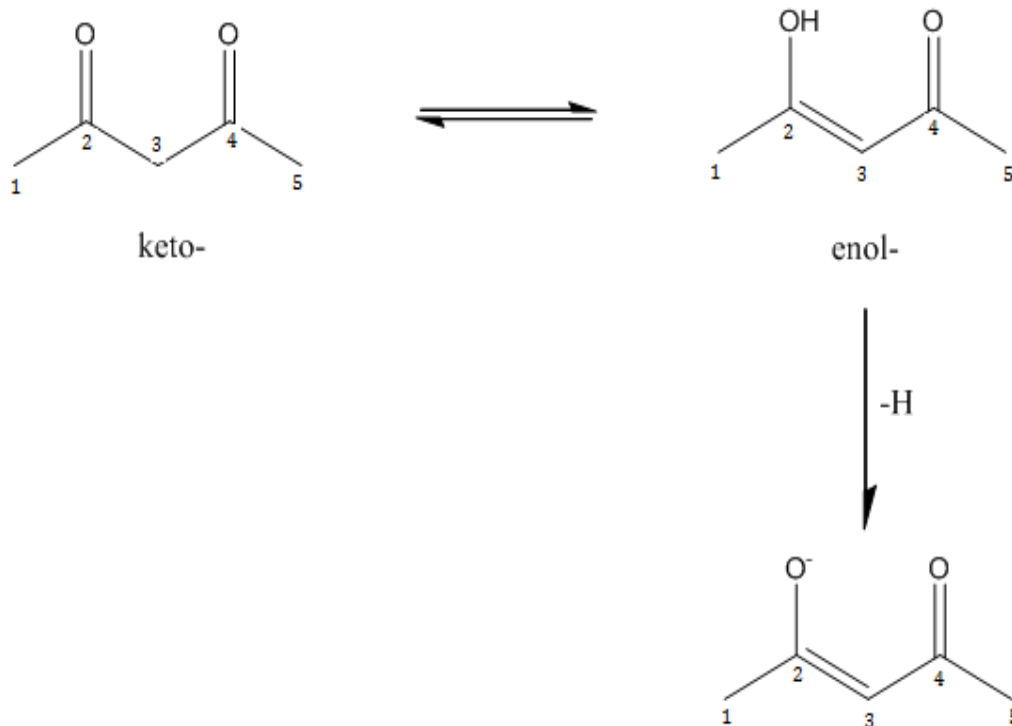


Figure 2.2: *diketone derivatives*

Acetylacetonate is used in the production of anti-corrosion agents and its peroxide compounds for radical initiator application for polymerization. It is used as a chemical intermediate in the production of drugs and pesticides.¹⁷ Acetylacetonate is a very strong base, it can deprotonate into two carbonyl groups and results in alkylation at C₁ (carbon one). Arylation is also obtained by substitution of halides on benzoic acid.¹⁸

Acetylacetonate can be converted to heterocycles to pyrazoles with hydrazine and to pyrimidines with urea.¹⁹ Acetylacetonate condenses with amines to give diketamine²⁰ and can also be used in the preparation of metal acetylacetonates for catalyst application.²¹ e.g. bis(acetylacetonato)oxovanadium(IV).

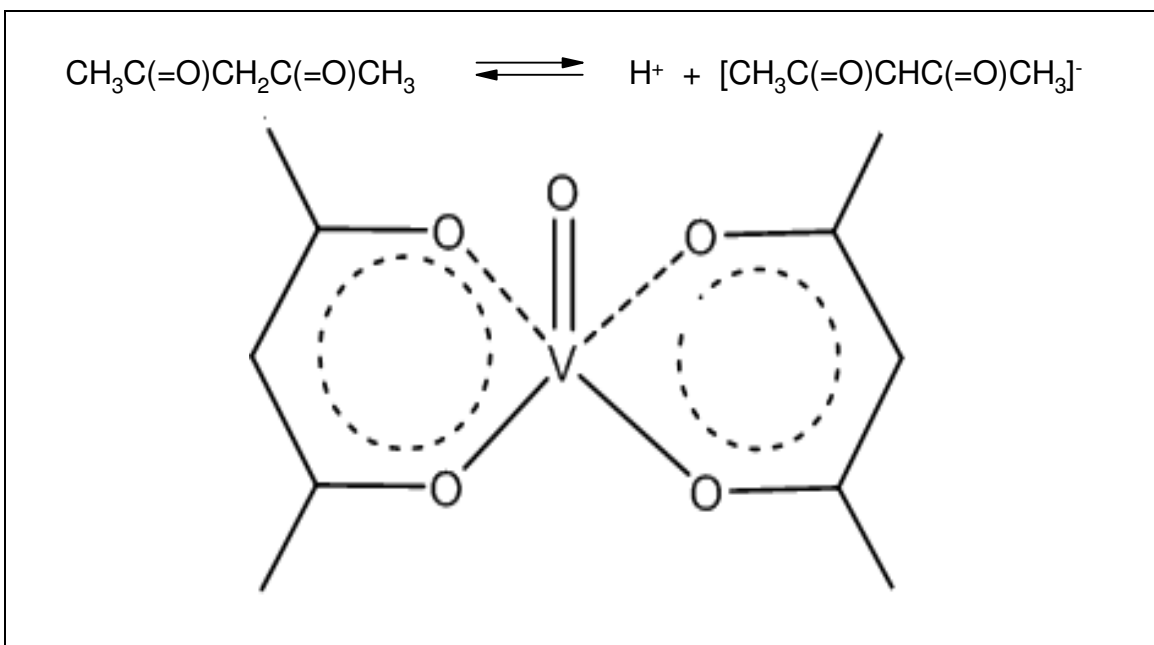


Figure 2.3: *bis(acetylacetonato)oxovanadium(IV)*

2.3 CARBON NANOMATERIALS

The carbon element is the most versatile element in the periodic table and can form a number of bonds with many different elements. The properties of carbon are a direct consequence of the arrangement of electrons around the nucleus²²⁻³³ i.e. ${}^6\text{C}$, $1s^2 2s^2 2p^2$ orbitals

Covalent bonds are formed by promoting the 2s electrons to the 2p orbitals resulting in the hybridization of the orbitals.²⁴ There are three ways of orbital hybridization:

- The 2s orbital pairs up with one of the 2p orbitals, forming two hybridized sp^1 orbitals in a linear geometry, separated by an angle of 180° .²⁵
- The 2s orbital hybridizing with two 2p orbitals resulting in three sp^2 orbitals, in the same plane separated by 120° .²⁶

- One 2s orbital hybridizes with the three 2p orbitals yielding four sp^3 orbitals separated by 109.5° .²⁷

In all these three ways above, the energy required to hybridize the atomic orbitals is given by the free energy of forming chemical bonds with other atoms.²⁸ Carbon can form a sigma (σ) or a pi (π) bond or both during the formation of a molecule.²⁹ The molecular structure depends on the level of hybridization of the carbon orbitals. The number and nature of the bonds determine the geometry and properties of carbon allotropes.²⁹

- Sp^1 hybridized carbon atom can make two σ bonds and two π bonds.
- Sp^2 hybridized carbon atom forms three σ bonds and one π bond.
- Sp^3 hybridized carbon atom forms four σ bonds.

There are a number of carbon nanomaterials that have been discovered over the past years such as carbon nanotubes (CNT`s), nanofibers, nano-anions, nanocapsules, and carbon nanospheres (CNS) that results from carbon`s ability to hybridize sp , sp^2 and sp^3 bonds.³⁰

2.3.1 Carbon nanotubes

CNT`s are a new form of carbon that is formed from hexagonal arrays of carbon atoms.³¹⁻³² CNT`s have concentric graphitic cylinders open at each end with five-membered rings present in it and carbon atoms tiling on a spherical or nearly

spherical surfaces.³³ The synthesis of CNT`s have become of high interest in the field of carbon nanomaterials after the discovery of fullerene.³⁴

The nature of the bonding of a CNT`s are described by applied quantum chemistry, specifically, orbital hybridization.²⁷⁻³³ The chemical bonding of CNT`s are composed entirely of sp^2 bonds, similar to those of graphite. This bonding structure, which is stronger than the sp^3 bonds found in diamonds, provides the molecules with their unique strength.²⁷ CNT`s naturally align themselves into ropes and are held together by Van der Waals forces.³⁴

CNT`s have a very small particle size that is measured in nanometers.³⁵ CNT`s possess some very unique characteristics due to their hollow center, nanometer size, large surface area and are able to change their electrical resistance drastically when exposed to alkalines and halogens at room temperature.³⁶

The cylindrical carbon molecules have novel properties that make them potentially useful in many applications in nanotechnology³⁷ e.g. in electrodes of fuel cell, battery storage, reinforcement of polymer, solar cell, air filters, artificial muscles, batteries, field emission, flat panel displays, data storage, magnetic nanotube, molecular quantum wires, hydrogen storage, noble radioactive gas storage, solar storage, waste recycling, electromagnetic shielding, dialysis filters, thermal protection, nanotube reinforced composites, collision-protection materials and fly wheels.³⁸⁻³⁹

There are several types of CNT`s such as single-wall carbon nanotubes (SWCNT`s) and multi-wall carbon nanotubes (MWCNT`s).⁴⁰

2.3.1.1 Single-wall carbon nanotubes

SWCNT`s are considered as a sheet of graphene rolled up into a seamless cylinder with a singular graphene cylindrical wall (as presented in Figure 2.4).⁴¹ SWCNT`s have a high ability to predict nanotubes properties based on their theoretical structure and are relatively simple compared to other nanotubes.⁴² Most SWCNT`s have a diameter of about 1 nm, with a tube length that can be a few microns longer. The structure of a SWCNT`s can be conceptualized by wrapping one atom thick layer of graphite called graphene into a seamless cylinder.⁴³

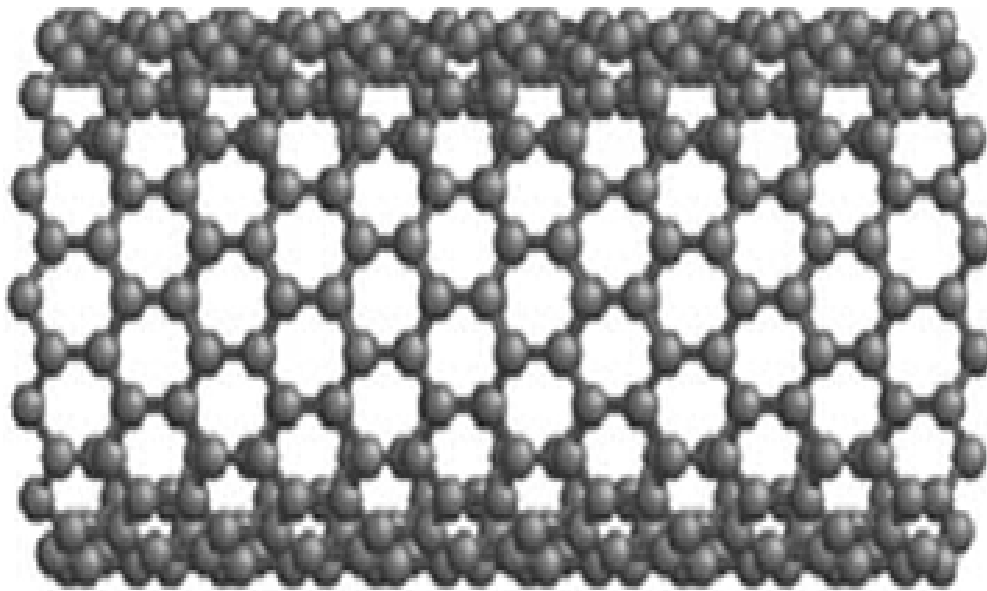


Figure 2.4: SWCNT`s with singular graphene cylindrical walls.⁴⁴

The way that the graphene sheet is wrapped is represented by a pair of indices (n,m) called the chiral vector.⁴⁵ The integers n and m denote the number of unit vectors along two directions in the honeycomb crystal lattice of graphene. If $m = 0$, the

nanotubes are called zigzag. If $n = m$, the nanotubes are called armchair.⁴⁶ The diameter of a nanotube can be calculated from its (n, m) indices as follows:

$$d = \frac{a}{\pi} \sqrt{(n^2 + nm + m^2)}.$$

where $a = 0.246$ nm.

SWCNT`s are an important variety of CNT`s because they exhibit electric properties that are not shared by the MWCNT variants.⁴⁵ In particular, their band gap can vary from zero to 2eV and their electrical conductivity can show metallic or semiconducting behavior, whereas MWCNTs are zero-gap metals.⁴⁷ SWCNT`s are the most likely candidate for miniaturizing electronics beyond the micro electromechanical scale currently used in electronics.⁴⁸ The most basic building block of these systems is the electric wire, and SWCNTs can be excellent conductors.⁴⁴ One useful application of SWCNT`s is in the development of the first intermolecular field effect transistors (FET).⁴⁹

2.3.1.2 Multi-wall carbon nanotubes

MWCNT`s are considered as sheets of graphene that had been rolled up into a seamless cylinder with multi graphene cylindrical wall.⁴⁰ MWCNT`s have a central tube of nanometric diameter surrounded by graphitic layers that is separated by ~0.34 nm with a well defined shape, composition, high aspect ratio, mechanically robust, excellent wear properties and chemical functionalization at the tip (**as presented in Figure 2.5**).⁵⁰

MWCNT`s can undergo transverse vibrations. MWCNT`s of length consisting of n nanotubes of cylindrical shape is considered.⁴⁸ It lies on a Winkler foundation of modulus and is subject to an axial stress which can be tensile or compressive in which case is less than the critical buckling load.⁴⁶

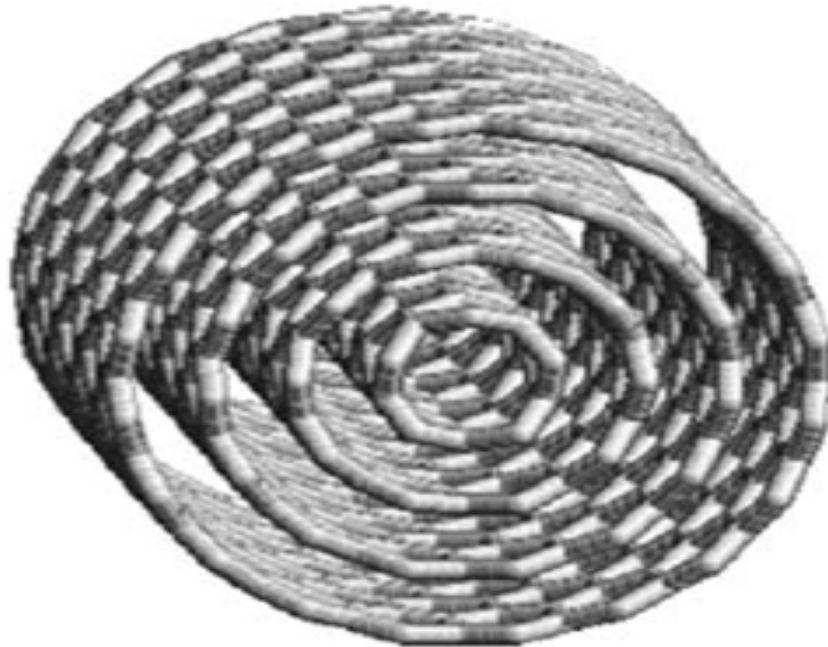


Figure 2.5: *MWCNT`s with multi layers of graphene cylindrical walls.*⁵¹

2.3.2 Carbon nanospheres

CNS`s results from the sp^2 hybridization of the carbon bond. CNS`s structure differs from other carbon nanostructures, they have a spherical structure or enclosed grapheme layers whereas CNT`s, nano-anions or nanocapsule have a tubular structure that is open on each end.⁵²

CNS`s posses some very unique chemical and physical properties. CNS`s have low density, high porosity and surface area, high chemical and thermal stability, and the ability to store large amount of hydrogen, making them useful for many applications.⁵³ CNS`s are mostly used in magnetic data storage,⁵⁴ catalysis,⁵⁵ magnetic resonance imaging⁵⁶ and biomedical applications.⁵⁷ CNS`s can be produced via the catalytic chemical vapor deposition (CCVD) synthesis method in two ways:

1. by a non-catalytic method or,
2. a catalytic method

2.4 SYNTHESIS METHODS

A number of methods have been developed to synthesize nanomaterials and those methods are: catalytic chemical vapor deposition (CCVD), arc-discharge, laser ablation and nebulizer spray pyrolysis (NSP).⁵⁸

2.4.1 Catalytic chemical vapor deposition

CCVD is a chemical process that is used to produce high-purity, high-performance solid materials. The process is often used in the semiconductor industry to produce thin films.⁵⁹ In a typical CCVD process, the substrate is exposed to one or more volatile precursors, which react and decompose on the substrate surface to produce the desired deposit. Frequently, volatile by-products are also produced, which are removed by gas flow through the reaction chamber. The nanotubes are grown from

nucleation sites of a catalyst in carbon based gas environments at elevated temperatures (600 – 1000 °C).⁶⁰

Micro-fabrication processes widely use CCVD to deposit materials in various forms, including: monocrystalline, polycrystalline, amorphous, and epitaxial. These materials include: silicon, carbon fiber, carbon nanofibers, filaments, carbon nanotubes, SiO₂, silicon-germanium, tungsten, silicon carbide, silicon nitride, silicon oxynitride and titanium nitride.⁶¹ The CCVD process is also used to produce synthetic diamonds.

❖ Advantages of the CCVD process are:

- Versatile technique for the production of CNT`s
- CNT`s can be made continuously, which provides a good way to synthesize large quantities of CNT`s under relatively controlled conditions.
- Expectation to strongly reduce the production costs since it is easy to scale up and suitable for continuous operation.⁶²⁻⁶³

There are different types of CCVD process. Their process differs according to their activation process and process condition. These are:

❖ Classified by operating pressure

- Atmospheric pressure CCVD (APCCVD) - CCVD processes at atmospheric pressure.
- Low-pressure CCVD (LPCCVD) - CCVD processes at sub-atmospheric pressures. Reduced pressures tend to reduce unwanted gas-phase

reactions and improve film uniformity across the wafer. Most modern CCVD processes are either (LPCCVD) or ultrahigh vacuum catalytic chemical vapor deposition (UHVCCVD).⁶⁵

- UHVCCVD - CCVD processes at a very low pressure, typically below 10^{-6} Pa ($\sim 10^{-8}$ torr). Note that in other fields, a lower division between high and ultra-high vacuum is common, often 10^{-7} Pa.⁶⁶

❖ Classified by physical characteristics of vapor

- *Aerosol assisted CCVD* (AACCCVD) - A CCVD process in which the precursors are transported to the substrate by means of a liquid/gas aerosol, which can be generated ultrasonically. This technique is suitable for use with non-volatile precursors.⁶⁷
- *Direct liquid injection CCVD* (DLICCCVD) - A CCVD process in which the precursors are in liquid form (liquid or solid dissolved in a convenient solvent).⁶⁸ Liquid solutions are injected in a vaporization chamber towards injectors (typically car injectors). Then the precursor vapors are transported to the substrate as in classical CCVD process. This technique is suitable for use on liquid or solid precursors.⁶⁹ High growth rates can be reached using this technique.

❖ Plasma methods (see also Plasma processing)

- Microwave plasma-assisted CCVD (MPCCVD)
- Plasma-Enhanced CCVD (PECCVD) - CCVD processes that utilize plasma to enhance catalytic chemical reaction rates of the precursors.⁶⁹ PECCVD processing allows deposition at lower

temperatures, which is often critical in the manufacture of semiconductors.⁷⁰

- Remote plasma-enhanced CCVD (RPECCVD) - Similar to PECCVD except that the wafer substrate is not directly in the plasma discharge region. Removing the wafer from the plasma region allows processing temperatures down to room temperature.⁷¹
- ❖ Atomic layer CCVD (ALCCVD) – Deposits successive layers of different substances to produce layered with crystalline films.⁷²⁻⁷³
- ❖ Combustion Chemical Vapor Deposition (CCVD) - nGimat's proprietary Combustion Chemical Vapor Deposition process is an open-atmosphere, flame-based technique for depositing high-quality thin films and nanomaterials.⁷⁴
- ❖ Hot wire CCVD (HWCCVD) - also known as catalytic CVD (Cat-CVD) or hot filament CCVD (HFCCVD). Uses a hot filament to chemically decompose the source gases.⁷⁵
- ❖ Metal organic chemical vapor deposition (MOCVD) - CCVD processes based on metal organic precursors.⁷⁶
- ❖ Hybrid Physical-Chemical Vapor Deposition (HPCVD) - Vapor deposition processes that involve both chemical decomposition of precursor gas and vaporization of a solid source.⁷⁷
- ❖ Rapid thermal CVD (RTCVD) - CVD processes that use heating lamps or other methods to rapidly heat the wafer substrate. Heating only the substrate rather than the gas or chamber walls helps reduce unwanted gas phase reactions that can lead to particle formation.⁷⁵⁻⁷⁹

2.4.2 Arc-discharge method

With arc-discharge method, carbon nanotubes are produced by vaporization of graphite rods placed end-to-end in an arc-discharge chamber.⁸⁰ These rods are usually separated by a distance of 1 mm in an enclosure or chamber filled either with an inert gas such as argon or helium.⁸¹ Non-inert gases such as nitrogen and hydrogen are also used. The chosen gas is generally regulated at low pressure between 50 and 700 mbar.⁸² Upon introduction of a direct current (50 to 100 A) driven by a direct voltage of 20 V, high temperature arc-discharge is created between two electrodes.⁸³

This discharge vaporizes the positive carbon rod and the carbon vapor forms hot plasma, which is deposited on the negative electrode, the deposit eventually forms tubular structures called carbon nanotubes.⁸²⁻⁸³ Variation of temperature and catalyst density is believed to have an effect on the diameter of tubes produced by this method. Although the arc-discharge is considered as a simpler way of producing nanotubes, this technique produces a mixture of single and multi-walled carbon nanotubes depending on the catalyst used.⁸⁴ In addition; these nanotubes are contaminated with amorphous carbon and catalytic metal particles.

2.4.3 Laser ablation method

The laser ablation method is similar to the arc-discharge; both methods use graphite rods as the carbon source, however there is one difference between the two methods.⁸⁵ The arc-discharge method uses high temperature to vaporize the positive

graphite rod, while the laser method employs a pulse or continuous laser to vaporize the graphite rod into carbon atoms.⁸⁶ Single wall nanotubes are mostly produced by this method. Laser ablation method is however expensive since it requires high power and expensive laser.⁸⁵

2.4.4 Nebulizer spray pyrolysis (NSP)

NSP is one of the methods used in the synthesis of multi-walled carbon nanotubes.⁸²⁻⁸⁴ It's a form of chemical vapor deposition method but the difference is in the introduction of the catalyst and carbon sources. In the NSP, the catalyst is mixed together with a carbon source and the carbon source is normally a hydrocarbon solvent.⁸⁵ The mixture is atomized to generate a spray by means of an ultrasonic atomizer at frequencies between 100 kHz and 10MHz. this forms a spray which is carried through a quartz tube placed in the oven by an inert carrier gas.⁸⁶ The advantage of this technique over the CCVD method is that the nanotubes produced by this technique are well aligned, diameter and quality of nanotubes can be controlled by varying analysis parameters.⁸⁷ NSP produces nanotubes with little or no amorphous carbon impurities compared to the ordinary CCVD technique and other synthetic methods.⁸⁶

REFERENCES

1. D.A. Steinhurst, A.P. Baronavski, J.C. Owrutsky, *Chem. Phys. Lett.* 361 (2002) 513-519.
2. O. Grazani, L. Toupet, J.R. Hamon, M. Tilset, *J. Organomet. Chem.* 669 (2003) 200-206.
3. L.H. Ngai, F.E. Stafford, L. Schafer, *J. Am. Chem. Soc.* 91 (1969) 48.
4. J. Brunvoll, S.J. Cyvin, L. Schafer, *J. Organomet. Chem.* 27 (1971) 69.
5. L. Schafer, J.F. Southern, S.J. Cyvin, J.J. Brunvoll, *Organomet. Chem.* 24 (1970) 13.
6. J.T.S. Andrews, E.F. Westrum, N. Bjerrum, *J. Organomet. Chem.* 17 (1969) 293-302.
7. Z. Konya, I. Vesselenyi, K. Niesz, A. Kukovecz, A. Demortier, *Chem. Phys. Lett.* 360 (2002) 429.
8. E.L. Muetterties, J.R. Bleeke, E.J. Wucherer, T.A. Albright, *Chem. Rev.* 82 (1982) 499.
9. M.M. Jones, *J. Am. Chem. Soc.* 81 (1959) 3188.
10. J. Liu, M. Shao, X. Chen, W. Yu, X. Liu, Y. Qian, *J. Am. Chem. Soc.* 125 (27) (2003) 8088-8089.
11. J.A. Craig, E.W. Harlan, B.S. Snyder, M.A. Whitener, R.H. Holm, *Inorg. Chem.* 28 (1989) 2082.
12. A. Lehtonen, M. Wasberg, R. Sillanpaa, *Eur. J. Inorg. Chem.* 25 (2006) 767.
13. S. Velusamy, M. Ahamed, T. Punniyamurthy, *Org. Lett.* 6 (2004) 4821.
14. R. Purschel, E. Lassner, R. Scharf, *Anal. Chem.* 163 (1958) 104.
15. M.P. Pileni, B.W. Ninham, T. Gulik-Krzywichi, J. Tanori, I. Lisiecki, A. Filankembo, *Adv. Mat.* 11 (1999) 1358.

16. L.M. Qi, J.M. Ma, H.M. Cheng, Z.G. Zhao, *J. Phys. Chem. B.* 101 (1997) 3460.
17. Y.G. Sun, B. Mayers, Y.N. Xia, *Adv. Mat.* 15 (2003) 641.
18. Y. Kim, T. Mitani, *J. Cat.* 238 (2006) 394.
19. B.M. Babic, Lj.M. Vracar, V. Radmilovic, N.V. Krstajic, *Electrochim. Acta.* 51 (2006) 3820.
20. W. Caminati, J.U. Grabow, *J. Am. Chem. Soc.* 128 (3) (2006) 854-857.
21. G.D. Straganz, A. Glieder, L. Brecker, D.W. Ribbons, W.J. Steiner, *Biochem.* 369 (2003) 573-581.
22. Z. Zhou, S. Wang, W. Zhou, G. Wang, L. Jiang, W. Li, S. Song, J. Liu, G. Sun, Q. Xin, *Chem. Communication.* (2003) 394.
23. S. Iijima, *Nature.* 354 (7) (1991) 56-58.
24. S. Ndwandwe, P. Tshibangu, E.D. Dikio, *Int. J. Electrochem. Sci.* 6 (2011) 749-760.
25. Y.T. Jang, S.I. Moon, J.H. Ahn, Y.H. Lee, B.K. Ju, *Sens. Act. B.* 99 (2004) 118-122.
26. M.S. Dresselhaus, Y.M. Lin, O. Rabin, A. Jorio, A.G. Souza Filho, M.A. Piment, R. Saito Ge, G. Samsonidze, G. Dresselhaus, *Mat. Sci. Eng.* 23 (2003) 129-140.
27. H. Yang, S.C. Wang, D.L. Akins, *Chem. Phys. Lett.* 416 (2005) 18-21.
28. H. Dai, *Surf. Sci.* 500 (2002) 218-241.
29. M.S. Dresselhaus, G. Dresselhaus, R. Saito, *Carbon.* 33 (7) (1995) 883-891.
30. R.R. He, H.Z. Jin, Y.J. Yan, X.H. Chen, *Chem. Phys. Lett.* 298 (2) (1998) 170-176.
31. L.T. Chadderton, Y. Chen, *Phys. Lett. A.* 263 (4) (1991) 401-405.
32. J. Kong, A.M. Cassell, H. Dai, *Chem. Phys. Lett.* 292 (6) (1998) 567-574.
33. A. Rubio, J.L. Corkill, M.L. Cohen, *Phys. Rev. B.* 49 (1994) 5081-5084.
34. S. Karthikeyan, P. Mahalingam, M. Karthik, *E-J. Chem.* 6 (1) (2009) 1-12.

35. F. Kokai, A. Koshio, M. Shiraishi, T. Matsuda, S. Shimoda, M. Ishihara, Y. Koga, H. Deno, *Diam. Rel. Mat.* 14 (3) (2005) 724-728.
36. J.W. Mintmire, B.I. Dunlap, C.T. White, *Phys. Rev. Lett.* 68 (5) (1992) 631-634.
37. C. Dekker, *Phys. Tod.* 52 (5) (1999) 22-28.
38. R. Martel, V. Derycke, C. Lavoie, J. Appenzeller, K.K. Chan, J. Tersoff, P. Avouris, *Phys. Rev. Lett.* 87 (2001) 256805.
39. M.L. Cohen, *Mat. Sci. Eng. C.* 15 (2) (2001) 1-11.
40. E. Flahaut, R. Bacsa, A. Peigney, C. Laurent, *Chem Communication.* 12 (2003) 1442-1443.
41. C.S. Jayanthi, S.Y. Wu, *Phys. Rev. Lett.* 88 (2002) 217206.
42. M. Huhtala, A. Krasheninnikov, A. Kuronen, K. Nordlund, K. Kaski, *Phys. Rev. B.* 70 (2004) 245416.
43. B.M.I. Vander Zande, M.R. Bohmer, L.G.J. Fokkink, C. Schonenberger, *J. Phys. Chem. B.* 101 (1997) 852.
44. B.R. Martin, D.J. Dermody, B.D. Reiss, M.M. Fang, L.A. Lyon, M.J. Natan, T.E. Mallouk, *Adv. Mat.* 11 (1999) 1021.
45. F. Caruso, X. Shi, R.A. Caruso, A. Susa, *Adv. Mat.* 13 (2001) 740.
46. J.H. Enemark, C.G. Young, *Adv. Inorg. Chem.* 40 (1994) 2.
47. R.K. Kodama, *J. Magn. Mat.* 200 (1999) 359.
48. T. Oku, T. Hirata, N. Motegi, R. Hatakeyama, N. Sato, T. Mieno, N.Y. Sato, H. Mase, M. Niwano, M. Miyamoto, *J. Mat. Res.* 15 (2000) 2182.
49. H. Song, X. Chen. *Chem. Phys. Lett.* 374 (2003) 400.
50. S.W. Kim, M. Kim, W.Y. Lee, T. Hyeon, *J. Am. Chem. Soc.* 124 (2002) 7624.
51. S.J. Oldenburg, G.D. Hale, J.B. Jackson, N.J. Halas, *Appl. Phys. Lett.* 75 (1999) 1063.

52. R.E.I. Schropp, B. Stannowski, A.M. Brockhoff, P.A.T.T. van Veenendaal, J.K. Rath, *Mat. Phys. Mech.* (2002) 73-82.
53. X. Li, W.X. Chen, J. Zhao, W. Xiang, Z.D. Xu, *Carbon*. 43 (2005) 2168.
54. M.H. Rummeli, C. Kramberger, M. Loeffler, O. Jost, M. Bystrzejewski, A. Gruneis, T. Gemming, W. Pompe, B. Buechner, T. Pichler, *J. Phys. Chem. B*. 111 (2007) 8234.
55. M.H. Rummeli, M. Löffler, C. Kramberger, F. Simon, F. Fueleop, O. Jost, R. Schoenfelder, A. Gruneis, T. Gemming, W. Pompe, B. Buechner, T. Pichler, *J. Phys. Chem.* 111 (2007) 4094.
56. X. Lin, M.H. Rummeli, T. Gemming, T. Pichler, D. Valentin, G. Ruani, C. Taliani, *Carbon*. 45 (2007) 196.
57. M.H. Rummeli, E. Borowiak-Palen, T. Gemming, T. Pichler, M. Knupfer, M. Kalbac, L. Dunsch, O. Jost, S.R.P. Silva, W. Pompe, B. Buchner, *Nano Lett.* 5 (2005) 1209-1215.
58. W.L. Xu, T.H. Lu, C.P. Liu, W. Xing, *J. Phys. Chem. B*. 109 (2005) 14325.
59. X.Z. Xue, C.P. Liu, W. Xing, T.H. Lu, *J. Electro. Chem. Soc.* 153 (2006) 79.
60. E.D. Dikio, F.T. Thema, C.W. Dikio, F.M. Mtunzi, *Int. J. Nanotech. Appl.* 4 (2) (2010) 117-124.
61. H. Yang, P. Mercier, S.C. Wang, D.L. Akins, *Chem. Phys. Lett.* 416 (2005) 18-40.
62. J. Liu, M. Shao, X. Chen, W. Yu, X. Liu, Y. Qian, *J. Am. Chem. Soc.* 125 (27) (2003) 8088-8089.
63. M.P. Hogarth, G.A. Hards, *Platinum Mat. Rev.* 40 (1996) 150.
64. P.S. Kauranen, E. Skou, *J. Electroanal. Chem.* 408 (1996) 189.

65. X. Ren, S. Zelenay, S. Thomas, J. Davey, S. Gottesfeld, *J. Power Sources*. 86 (2000) 111.
66. B. Gurau, E.S. Smotkin, *J. Power Sources*. 112 (2002) 339.
67. T. Iwasita, F.C. Nart, *J. Electroanal. Chem.* 317 (1991) 291.
68. T.D. Jarvi, S. Sriramulu, E.M. Stuve, *J. Phys. Chem.* 101 (1997) 3646.
69. E. Redding, A. Sapienza, E.S. Smotkin, *Sci.* 280 (1998) 1735.
70. J. Kong, A.M. Cassell, H. Dai, *Chem. Phys. Lett.* 292 (6) (1998) 567-574.
71. W.X. Chen, J. Zhao, J.Y. Lee, Z.L. Liu, *Mat. Chem. Phys.* 91 (2005) 124.
72. M. Corrias, B. Caussat, A. Ayrat, J. Durand, Y. Kihn, *Chem. Eng. Sci.* 58(19) (2003) 4475-4482.
73. Z. Konya, I. Vesselenyi, K. Niesz, A. Kukovecz, A. Demortier. *Chem. phys. Lett.* 360 (2002) 429.
74. J. Bernholc, C. Roland, B.I. Yakobson, *Nano.* 2 (6) (1997) 706-715.
75. M. Corrias, B. Caussat, A. Ayrat, J. Durand, Y. Kihn, *Chem. Eng. Sci.* 58 (19) (2003) 4475-4482.
76. P. Benito, M. Herrero, F.M. Labajos, V. Rivers, C. Royo, N. Latorre, A. Monzon, *J. Chem. Eng.* 149 (2009) 455-462.
77. Q. Liang, Q. Li, L. Gao, Z. Yu, *J. Mat. Resear. Bull.* 36 (2001) 471-477.
78. R.R. He, H.Z. Jin, Y.J. Yan, X.H. Chen, *Chem. Phys. Lett.* 298 (2) (1998) 170-176.
79. R. long, R. Young, *J. Am. Chem. Soc.* 123 (2001) 2058.
80. S. Cui, P. Scharff, S. Siegmund, D. Schneider, K. Risch, S. klotzer, L. Spies, H. Romanus, J. Schawohl. *Carbon.* 42 (204) 931.
81. S. Durbach, N.J. Coville, M.J. Witcomb, *Carbon. Nano.* 12 (2005) 155.

82. L. Tapasztó, K. Kertész, Z. Vertesy, Z.E. Horváth, A.A. Koos, Z. Osvath, Z. Sarkózi, A. Darabont. L.P. Biro, *Carbon*. 43 (2005) 970.
83. S.R.C, Vivekchad, L.M. Cele, F.L. Deepack, A.R. Raju, A. Govindaraj, *Chem. Phys. Lett.* 386 (2002) 429.
84. H. Kuzmany, A. Kukovecz, F. Simon, M. Holzweber, C. Kramberger, T. Pichler, *Synth. Mat.* 141 (2004) 113.
85. X. Peng, Z. Luan, J. Dng, Z. Di, Y. Li, B. Tian, *Mat. Lett.* 59 (2005) 399.
86. K.L. Strong, D.P. Anderson, K. Lafdi, J.N. Kuhn, *Carbon*. 41 (2003) 1477.

3.1 INTRODUCTION

This chapter explains in details about the precursor preparations, reactions that took place, synthesis process, procedures, experimental techniques as well as instruments that were used in the execution of this research project. There was no standard technique modification that was done.

3.2 CHEMICALS AND MATERIALS

Most of the chemicals used in this project were reagents grade, some were purified as required. Solvents obtained at high purity from Sigma Aldrich were used as they were.

3.3 PREPARATION OF THE PRECURSORS

Bis(acetylacetonato)oxovanadium(IV), Manganese(III) acetylacetonate, Co-Zn and Co-Al were prepared and used as precursors for the production of carbon nanomaterials via the CCVD synthesis method. The precursors were prepared as follows:

3.3.1 Bis(acetylacetonato)oxovanadium(IV)

6 ml of distilled water, 4.6 ml of concentrated sulfuric acid, 12.6 ml of 95% ethanol and 2.5049 g of pure Vanadium (V) Oxide were added in an Erlenmeyer flask and mixed well together. The mixture was heated on a boiling water bath while stirring.

The slurry of Vanadium (V) oxide initial turned green and finally turned blue. The reaction took approximately 40 min. 10 ml of water was then added to the mixture and filtered by gravity and the filtrate was collected in a clean beaker. 6.6 ml of acetylacetonate was added to the filtrate in a beaker and stirred for 10 minutes and the mixture turned dark purple. The solution was then neutralized by slowly adding the mixture of 10.029 g of sodium carbonate and 60ml of water to the prepared solution, with continuous stirring to avoid excessive frothing.¹⁻⁴



The precipitated product was collected by filtration on a Buchner funnel and dried by drawing air through it.

3.3.2 Manganese(III) acetylacetonate

1 g of manganese (II) chloride, 2 g of sodium acetate and 4 ml of acetylacetonate were added to a conical flask containing 40 ml of water and stirred until the acetylacetonate was well dispersed. 10 ml of 0.125M potassium permanganate solution, 10 ml of water and 2 g sodium acetate were added to the prepared mixture. The mixture was heated in a steam bath until the purple potassium permanganate colour disappeared. The mixture was then filtered and the filtered precipitate left to dry.



The dried precipitate was dissolved in 15 ml of toluene and heated in a steam bath for 5 min to dissolve the Manganese acetylacetonate.²⁻³

3.3.3 Co-Zn and Co-Al

The precursor samples of Co-Zn and Co-Al were prepared by co-precipitation method described by Benito *et al*⁴ and by Liu⁵ *et al*. This was achieved by mixing cobalt and zinc for Co-Zn and, cobalt and aluminium for Co-Al at room temperature. The precipitates obtained were then washed to remove impurities and dried at 40°C in an open air oven.

3.4 CHARACTERIZATION OF CATALYST PRECURSORS

The catalyst precursors were characterized using the Fourier transformer infrared spectroscopy (FTIR). FTIR was used to determine the function groups present in the molecule or compound.

FTIR spectroscopy is one of the important tools used to identify functional groups that are present in a molecule or compound.⁶⁻⁸ In FTIR the infrared radiation causes excitation of electron within the molecule to vibrate because of its low energy. These vibrations may be symmetrical or asymmetrical depending on the types of atoms. The asymmetrical vibrations usually create a dipole within the molecule. Molecules with these types of vibrations absorb infrared radiation. Due to the differences in bond energies, different functional groups absorb infrared radiation at different wavelengths or energies,⁷ making it possible to identify different functional groups

present in the system as each functional group will absorb at a particular wavelength.

3.5 PRODUCTION OF THE CARBON NANOMATERIALS

Figure 3.1 shows a schematic diagram of the experimental procedure (CCVD). The reactor consisted of a 40 mm o.d x 70 cm long quartz tube heated by an electrical tube furnace with a temperature controller. Nitrogen gas flowing at 40 ml/min was passed through the reactor for approximately 70 min, after stabilization for 10 min, the nitrogen gas flow was maintained at 40 ml/min. The acetylene with a flow rate of 10 ml/min was passed for 60min through the reactor.⁹

The catalyst placed on a quartz boat was placed in the centre of the furnace during the synthesis.⁹ Flow rate of the gases was controlled by a mass flow controller (MFC). The temperature was maintained at 875°C during the reaction. After the reaction had taken place, the reactor was cooled to room temperature with nitrogen flowing at 40ml/min for 3 to 4 hrs.

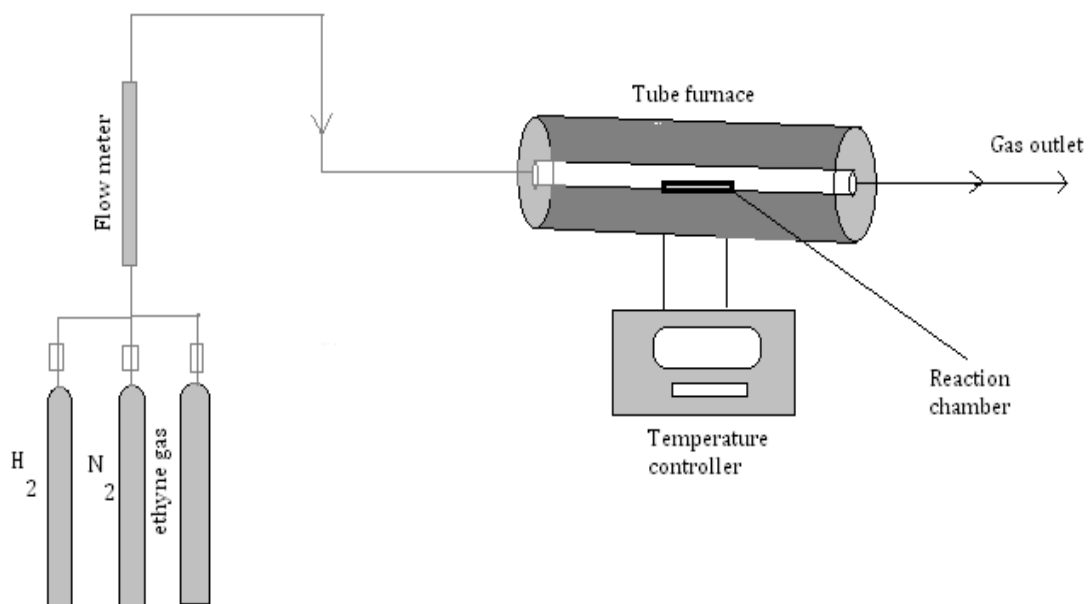


Figure 3.1 : schematic diagram of the CCVD process.⁹

3.6 CHARACTERIZATION OF CARBON NANOMATERIALS

The produced carbon nanomaterials properties were analyzed using Raman spectroscopy, Scanning electron microscopy (SEM), Energy dispersive spectroscopy (EDS), X-ray diffraction (XRD), Transmission electron microscopy (TEM) and Thermogravimetric Analysis (TGA).

3.6.1 Raman spectroscopy

The Raman spectra were obtained on a Raman spectroscope, Jobin-Yvon HR800 UV-VIS-NIR Raman spectrometer equipped with an Olympus BX 40 attachment. The excitation wavelength was 514.5 nm with an energy setting of 1.2 mV from a coherent Innova model 308 argon-ion laser. The Raman spectra were collected by

means of back scattering geometry with an acquisition time of 50 sec. The sample was illuminated with laser beam. Light from the illuminated spot was collected with a lens and sent through a monochromator. Wavelengths close to the laser line were filtered out while the rest of the collected light was dispersed onto the detector then the read out where the Raman spectra were observed. When processing the sample on the Raman spectroscopy the laser light interacts with photons, molecular vibrations or other excitations in the system resulting, in the energy of the laser photons being shifted up or down. The shift in energy gives information about the phonon modes in the system.¹⁰⁻¹³

3.6.2 Scanning electron microscopy

The SEM images were obtained using Philips XL30 scanning electron microscope with the image magnification range of X5-X200 000, a resolution of 2m and an accelerating voltage of 1-30keV. To obtain the SEM images, the electron beam was thermionically emitted from an electron gun fitted with a tungsten filament cathode allowing the electron beam to be heated for electron emission and interacts with the sample.¹⁴ When the electron beam interacted with the sample, the electrons lost energy by repeated random scattering and absorption within a teardrop-shaped volume of the specimen known as the interaction volume, which extended from less than 10nm to 5 μ m into the surface.¹⁴⁻¹⁵

3.6.3 Energy dispersive spectroscopy

The EDS measurements were recorded using a JEOL 7500F Field Emission scanning electron microscope. To stimulate the emission of characteristic X-rays from a specimen, a high-energy beam of charged particles focuses into the sample being studied. Initially, an atom within the sample contained unexcited electrons in discrete energy levels bounded to the nucleus.¹⁶⁻¹⁸ When the incident beam excite an electron in an inner shell, ejecting it from the shell while creating an electron hole where the electron was. An electron from an outer or higher-energy shell then fills the hole, and the difference in energy between the higher-energy shell and the lower energy shell is released in the form of X-ray.¹⁷

3.6.4 X-ray diffraction

Powder X-ray diffraction (PXRD) patterns were studied with a Bruker AXS D8 Advanced diffractometer operated at 45 kV and 40 mA with monochromated copper K α 1 radiation of wavelength ($\lambda = 1.540598$) and K α 2 radiation of wavelength ($\lambda = 1.544426$). Scan speed of 1 s/step and a step size of 0.03°.

3.6.5 Transmission electron microscopy

The HR-TEM images of the sample were obtained using a CM 200 electron microscope operated at 100 kV.

3.6.6 Thermogravimetric analysis

The thermal behavior of the carbon nanomaterials were investigated by TGA using a Q500 TGA instrument under an air environment. The prepared nanomaterial samples were heated in platinum crucibles with oxygen and nitrogen gases at a flow rate of 40 and 60 ml/min respectively. The dynamic measurement was made between ambient and 1000°C with a ramp rate of 10°C/min to 900°C.

TGA was used to study the thermal behavior of carbon nanomaterials with variations in heating temperature.¹⁸ Changes are associated with weight loss resulting from dehydration or decomposition of the sample with the increase in temperature. The weight loss can also arise from the formation of physical and chemical bonds that can lead to the release of volatile compounds.¹⁸

REFERENCES

1. J. Kong, A.M. Cassell, H. Dai, *Chem. Phys. Lett.* 292 (6) (1998) 567-574.
2. E. Redding, A. Sapienza, E.S. Smotkin, *Sci.* 280 (1998) 1735.
3. P.W. Atkins, J. de Paula, *Phys. Chem.* 7th ed. (2002) 481-524.
4. P. Benito, M. Herrero, F.M. Labajos, V. Rives, C. Royo, N. Latorre, A. Monzon, *J. Chem. Eng.* 149 (2009) 455-462.
5. J. Liu, M. Shao, X. Chen, W. Yu, X. Liu, Y. Qian, *J. Am. Chem. Soc.* 125 (27) (2003) 8088-8089.
6. H. Kuzmany, A. Kukovecz, F. Simon, M. Holzweber, C. Kramberger, T. Pichler, *Synth. Mat.* 141 (2004) 113.
7. X. Peng, Z. Luan, J. Dng, Z. Di, Y. Li, B. Tian, *Mat. Lett.* 59 (2005) 399.
8. R. long, R. Young, *J. Am. Chem. Soc.* 123 (2001) 2058.
9. E.D. Dikio, F.T. Thema, C.W. Dikio, F.M. Mtunzi, *Int. J. Nanotech. Appl.* 4 (2) (2010) 117-124.
10. S. Durbach, N.J. Coville, M.J. Witcomb, *Carbon. Nano.* 12 (2005) 155.
11. L. Tapasztó, K. Kertesz, Z. Vertesy, Z.E. Horvath, A.A. Koos, Z. Osvath, Z. Sarkozi, A. Darabont. L.P. Biro, *Carbon.* 43 (2005) 970.
12. S.R.C. Vivekchad, L.M. Cele, F.L. Deepack, A.R. Raju, A. Govindaraj, *Chem. Phys. Lett.* 386 (2002) 429.
13. K.L. Strong, D.P. Anderson, K. Lafdi, J.N. Kuhn, *Carbon.* 41 (2003) 1477.
14. Z. Konya, I. Vesselenyi, K. Niesz, A. Kukovecz, A. Demortier, *Chem. phys. Lett.* 360 (2002) 429.
15. M. Xu, T. Zhang, B. Gu, J. Wu, Q. Chen, *Macro. Molec.* 39 (2006) 3540-3545.
16. J. Xiong, Z. Zheng, X. Qin, M. Li, X. Wang, *Carbon.* 44 (2006) 2701-2707.

17. A. R. Khan, K. Stine, P. Forgo, V.T. D`Souza, *Chem. Rev.* 98 (1998) 1978.
18. J. Kong, A.M. Cassell, H. Dai, *J. Chem. Phys. Lett.* 292(6) (1998) 567-574.

4.1 INTRODUCTION

Results obtained from this study are presented and discussed in this chapter. This includes the results for characterization of catalyst precursor(s) using Fourier-Transform Infrared spectroscopy to determine their functional groups, and, the results for the characterization of carbon materials to obtain their nanostructures using Raman Spectroscopy, Scanning Electron Microscopy, Energy Dispersive Spectroscopy, X-ray Diffraction, Transmission Electron Microscopy and Thermogravimetric Analysis.

4.2 CHARACTERIZATION OF CATALYST PRECUSORS

Acetylacetonate used in the synthesis of metal acetylacetonates and synthesized metal acetylacetonates were analysed using the Fourier Transform Infrared spectroscopy (FTIR).

Figure 4.1 shows the FTIR spectrum of pure acetylacetonate. Acetylacetonate is a diketonate, having both the enol- and keto- form co-existing in a solution, hence there is a doublet for the asymmetric and symmetric stretching frequency observed at 1728.31 cm^{-1} and 1708.53 cm^{-1} respectively. The enol- form appears at 1708.53 cm^{-1} and the keto-form is observed at 1728.31 cm^{-1} but is shifted and intensified comparing to the normal ketone value at $1725\text{-}1705\text{ cm}^{-1}$. The shift results from an internal hydrogen bonding and also contributes to the lowering of the carbonyl frequency in the enol-form.

The relative intensities of the enol- and keto- carbonyl absorptions depend on the percentage present at equilibrium. To confirm the presence of the carbonyl group in a solution is an aromatic peak observed at 1604.13 cm^{-1} and the $-\text{CH}_3$ at 3005.84 cm^{-1} .

In Figure 4.2 is the FTIR graph of bis(acetylacetonato)oxovanadium(IV). A shifted peak of the enol- form (carbonyl group) is observed at 1588 cm^{-1} and the aromatic at 1516 cm^{-1} confirms the carbonyl group. The lowering of the carbonyl group and an aromatic frequency is caused by the hydrogen-bonding effect to a carbonyl group. The carboxylic acid peak observed at 3387.49 cm^{-1} also confirms the presence of the carbonyl group in a solution and the ester peak observed at 1356 cm^{-1} confirms the presence of the aromatic. The stretching vibration of the vanadyl bond is observed at 991 cm^{-1} . This is usually observed at $950\text{-}999\text{ cm}^{-1}$ for the six coordinate oxovanadium (V) complex. The in-plane vibration of the cyclic fragment is observed at 934 cm^{-1} while the out-of-plane bending vibrations are observed as a doublet at 788 and 797 cm^{-1} . In the range 1416 and $934\text{-}1112\text{ cm}^{-1}$, the FTIR spectrum exhibits bands that correspond to the CH_3 group. The spectrum has a strong sharp band which is assigned to a vibration that corresponds to the C-C-C angle at 1285 cm^{-1} .

The FTIR spectrum in Figure 4.3 is that of Manganese(III) acetylacetonate. A shifted peak of the keto- form (carbonyl group) is observed at 1567 cm^{-1} and an aromatic confirming the carbonyl group is observed at 1505.24 cm^{-1} . The lowering of the carbonyl group and aromatic frequencies is caused by the hydrogen-bonding effect to a carbonyl group. The ester peak appearing at 1338 cm^{-1} confirms the presence of an aromatic ring in the solution. The in-plane vibration of the cyclic fragment is

observed at 923 cm^{-1} while the out-of-plane bending vibration is observed at 774 cm^{-1} . In the range of $923\text{-}1190\text{ cm}^{-1}$, the FTIR spectrum exhibit bands corresponding to the CH_3 group.

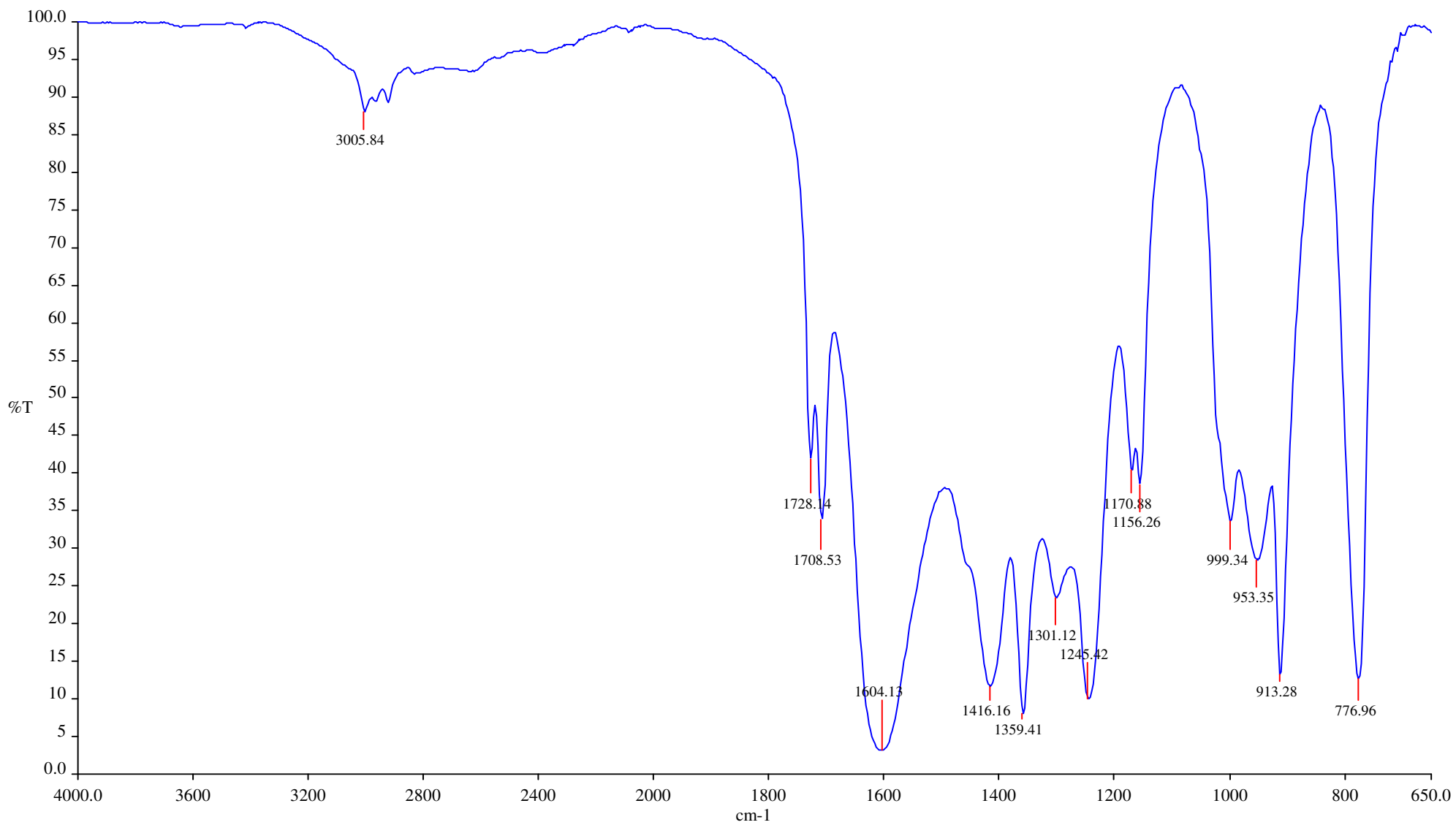


Figure 4.1: FTIR spectrum of pure acetylacetonate

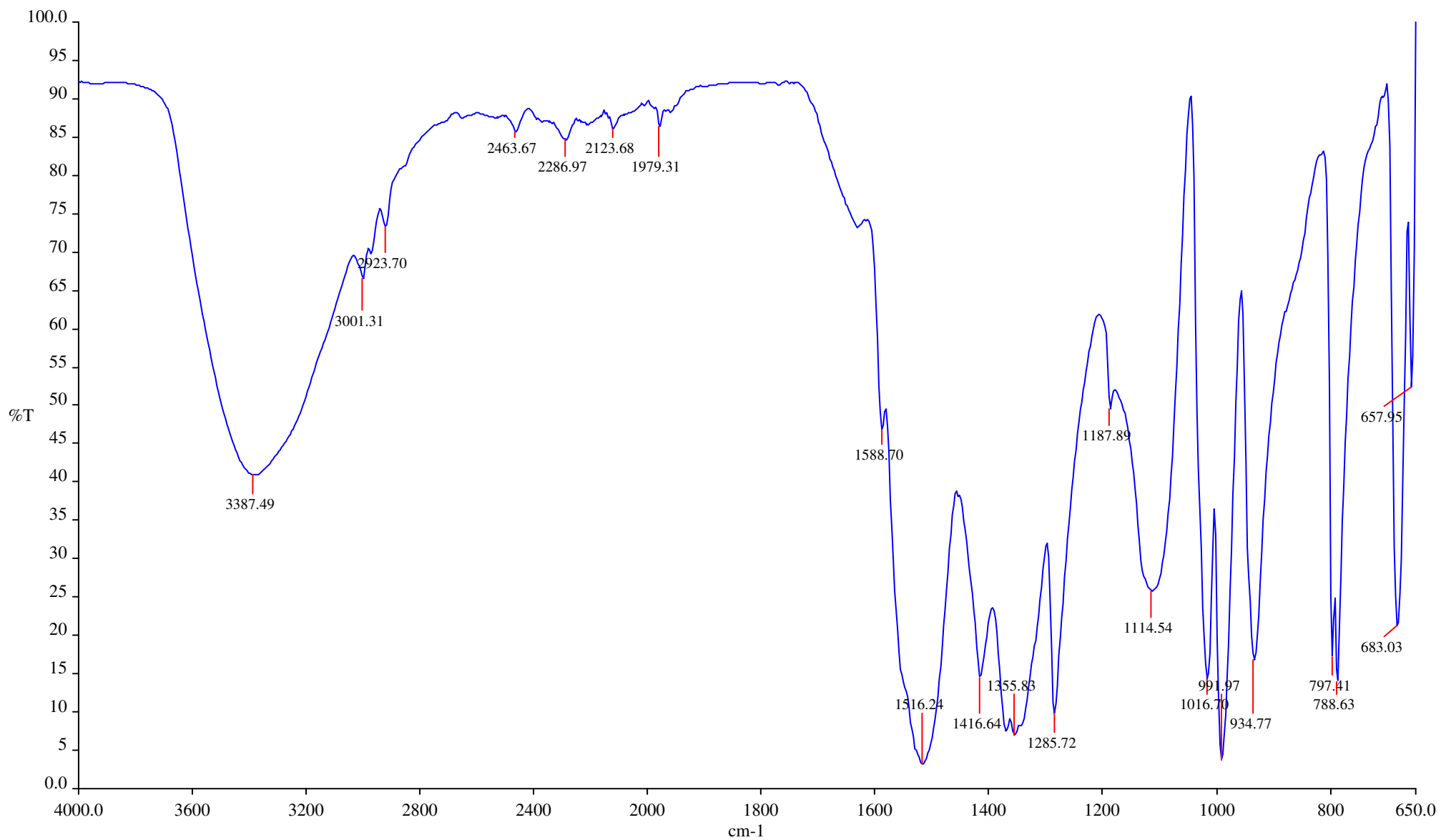


Figure 4.2: FTIR spectrum of bis(acetylacetonato)oxovanadium(IV)

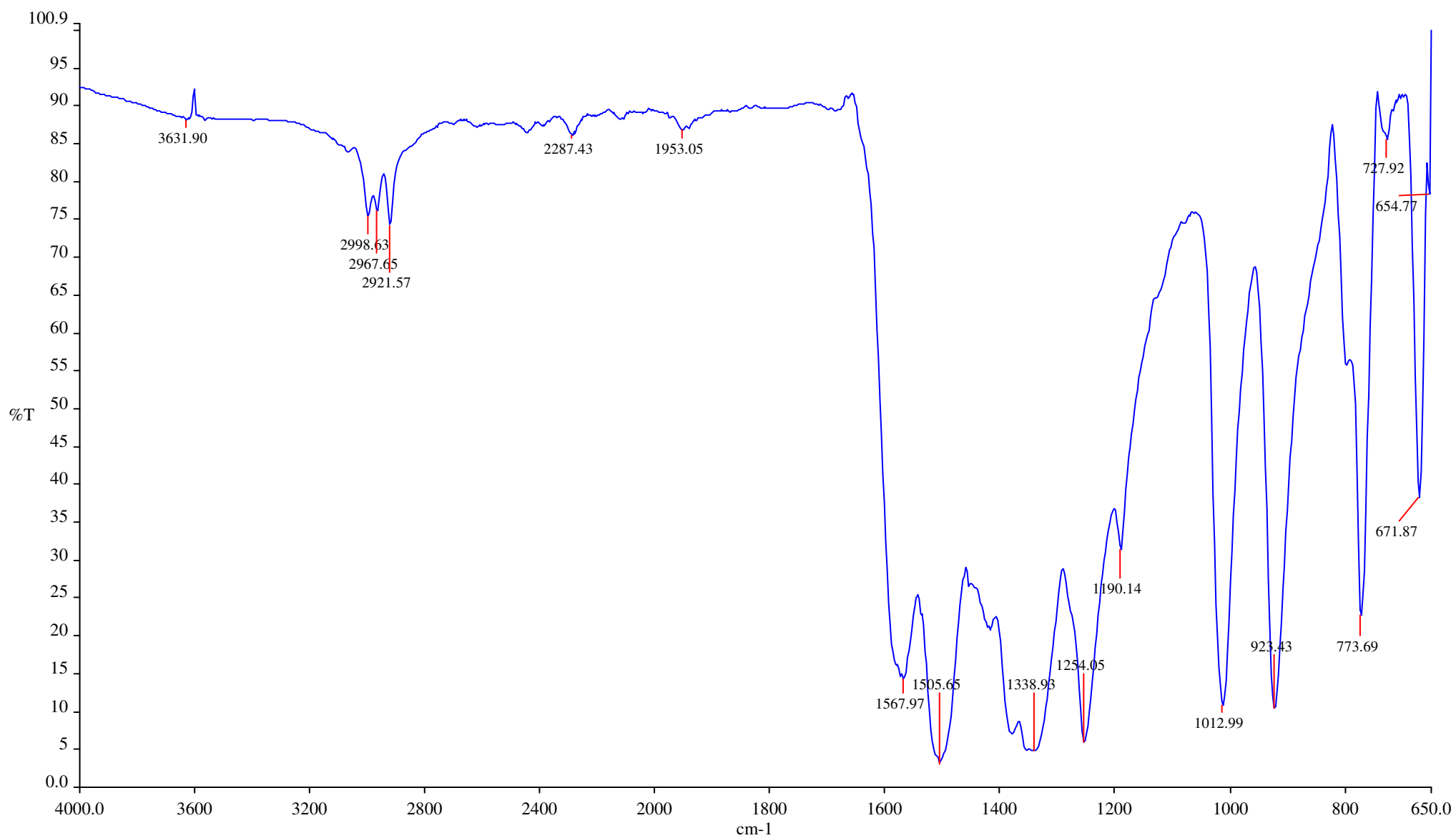


Figure 4.3: FTIR spectrum of Manganese(III) acetylacetonate

4.3 CHARACTERIZATION OF THE CARBON NANOMATERIALS

Bis(acetylacetonato)oxovanadium(IV), Manganese(III) acetylacetonate, Co-Zn and Co-Al were synthesized using the CCVD synthesis method to produce carbon materials. Carbon materials produced from the CCVD synthesis process were characterized using Raman Spectroscopy, Scanning Electron Microscopy, Energy Dispersive Spectroscopy, X-ray Diffraction, Transmission Electron Microscopy and Thermogravimetric Analysis.

4.3.1 Carbon nanomaterials as-prepared from bis(acetylacetonato)oxovanadium (IV)

Carbon materials as-prepared from bis(acetylacetonato)oxovanadium(IV) catalyst precursor were characterized using Raman Spectroscopy, Scanning Electron Microscopy, Energy Dispersive Spectroscopy, X-ray Diffraction, Transmission Electron Microscopy and Thermogravimetric Analysis.

Raman spectroscopy was used to study the vibration, rotation and other frequency modes in the system, as well as, to reveal several properties of carbon material. The Raman spectrum (**as presented in Figure 4.4**) of the synthesized bis(acetylacetonato)oxovanadium catalyst precursor shows several peaks at 1121.06, 1329.88, 1593.1, 2098.79, 2165.17 and 2671.79 cm^{-1} . The two major peaks: are the D- and G- bands which indicate the presence of crystalline graphitic carbon in the sample, these bands are observed at 1329.88 and 1593.1 cm^{-1} respectively. The D-band at

1329.88 cm^{-1} , has been attributed to the presence of amorphous carbon due and graphitic carbon whiles the G-band band at 1593.1 cm^{-1} is that of ordered carbon materials.

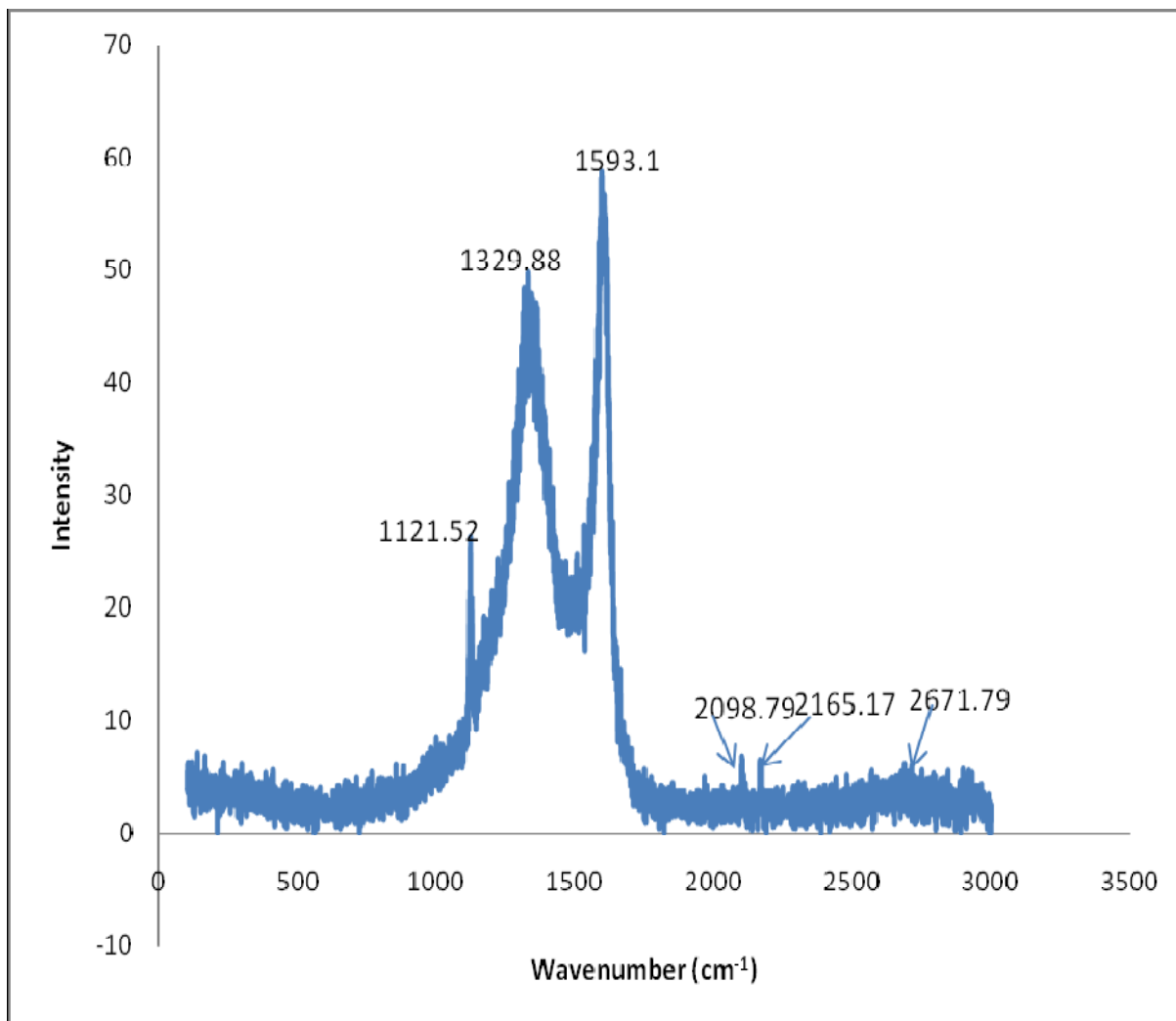


Figure 4.4: Raman spectrum of carbon material prepared from bis(acetylacetonato)oxovanadium (IV)

The G- band at 1593.1 cm^{-1} correspond to an E_{2g} mode of graphite which is related to the vibration of sp^2 bonded carbon atoms and the presence of ordered carbon material in a sample. The strength of the D-band can be identified with wall disorder or the presence of coating on the outside of spheres. The peak at 1121.06 cm^{-1} is the T-band

and is due to an amorphous carbon. A notable observation in this spectrum is the absence of an overtone peak that should have resonated at about 2600 cm^{-1} from the D- and G- bands. A small peak is however observed at about 2671.79 cm^{-1} with an intensity of 5.2084. The absence of this peak could be related to the amount of carbon material produced in the synthesis as well as their purity. The intensity ratio of these two bands ($I_D/I_G = 0.8556$) is considered as a parameter to determine the quality of carbon material in the sample, with a high intensity ratio indicating a high degree of disorder in carbon material. The intensity ratio for the two peaks is 0.8556 indicating a high quality of carbon material obtained during the synthesis.

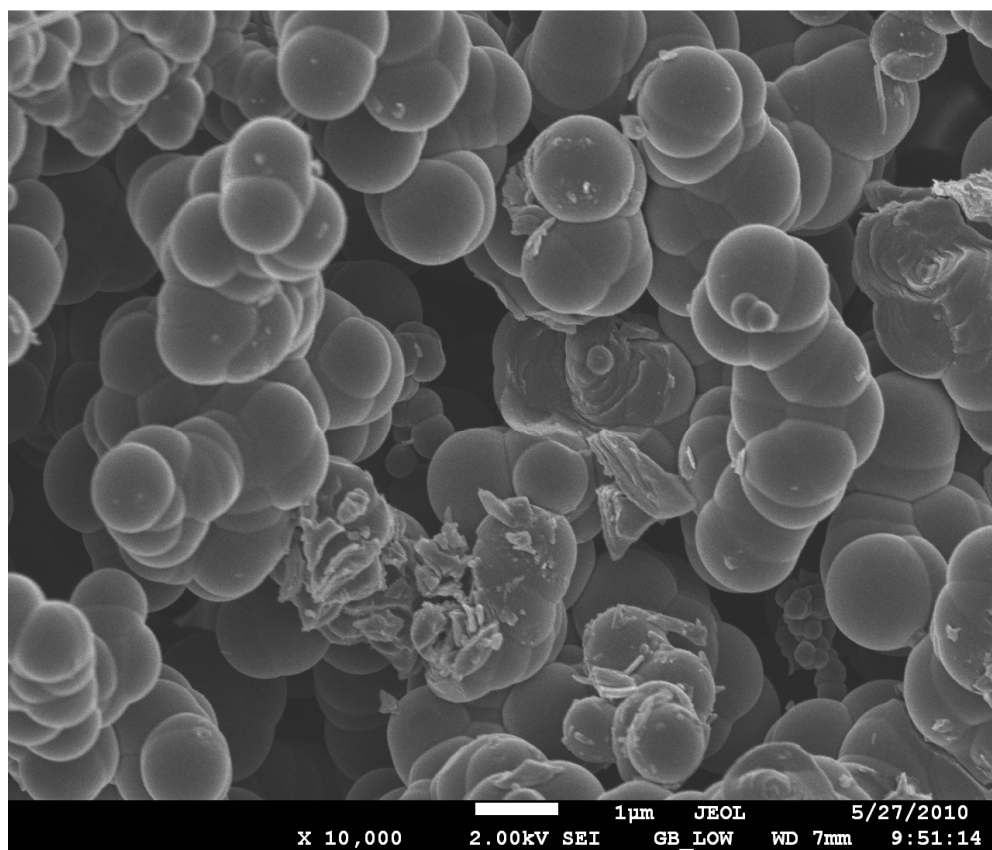


Figure 4.5: SEM image of carbon material as-prepared from bis(acetylacetonato)oxovanadium(IV)

Scanning Electron Microscopy (SEM) was used to determine the shape and size of the particles synthesized. The SEM image of the as-prepared carbon material is presented in Figure 4.5. The surface morphology of the carbon deposit is seen to form several spherical particles which can be called carbon spheres. It can be seen that these spheres are relatively uniform with a diameter of about $104\mu\text{m}$. The spheres are seen to agglomerate together forming a chain. There are a few broken spheres observed in Figure 4.5 which may have been caused by magnetostatic energy of the particles.

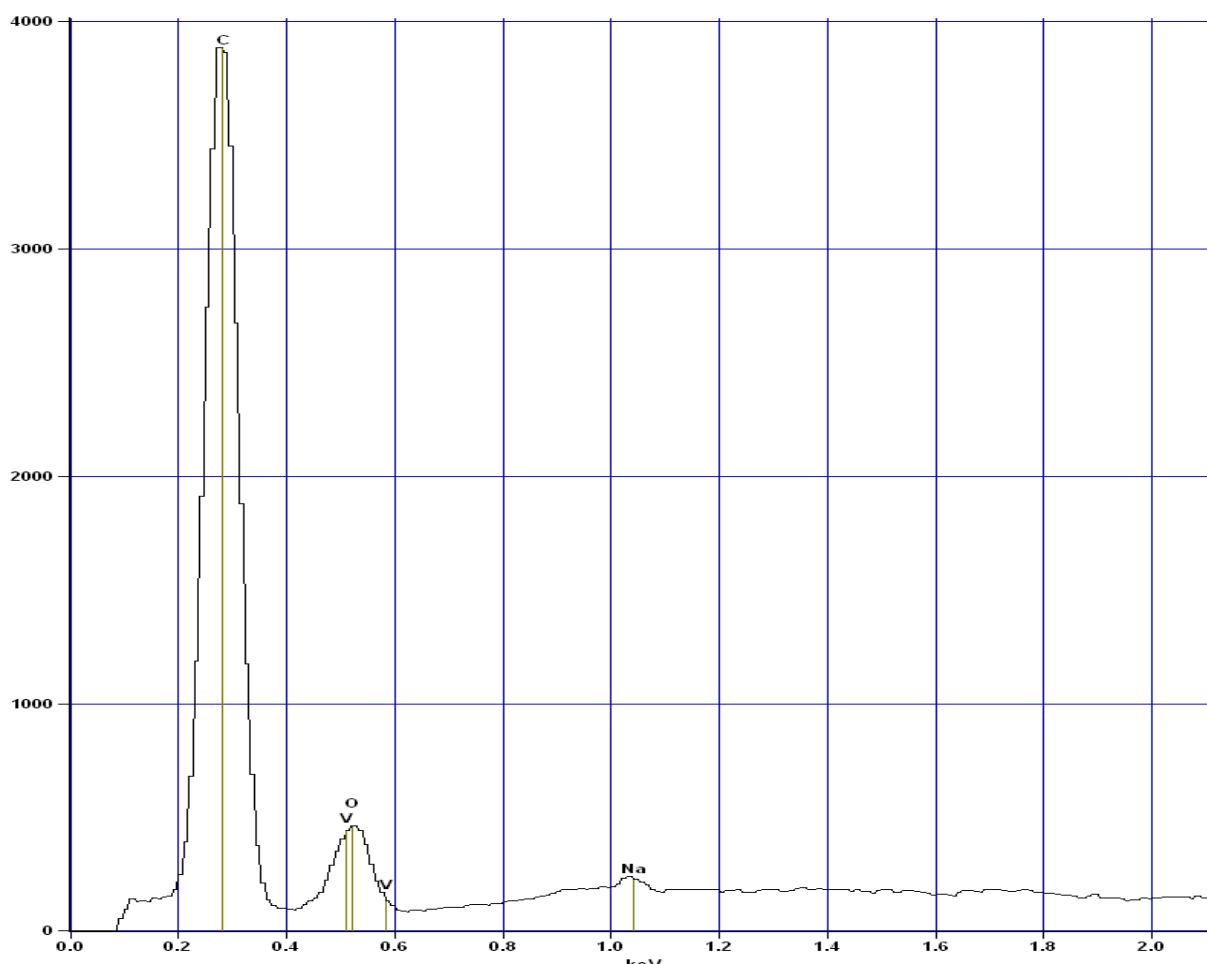


Figure 4.6: EDS spectrum of carbon material as-prepared from bis(acetylacetonato)oxovanadium(IV)

Energy dispersive spectroscopy (EDS) is not a quantitative technique but the intensities observed are an indication of relative quantities of the identified components in a sample. EDS was used to determine the elemental composition of the emitted X-rays versus their energy levels. The EDS spectrum of carbon spheres formed from the synthesized bis(acetylacetonato)oxovanadium (IV) catalyst precursor is presented in Figure 4.6. The spectrum shows the presence of carbon, oxovanadium (V=O), vanadium and sodium at 0.3, 0.5, 0.58 and 1.02 KeV respectively. The spectrum in Figure 4.6 shows carbon as well as the catalyst precursor's metals. The carbon is derived from the carbon spheres while oxovanadium and sodium are derived from the catalyst precursor.

X-ray diffraction (XRD) pattern of the as-prepared carbon spheres is shown in Figure 4.7. Bragg diffraction peaks at $2\theta = 25.29^\circ$, 33.14° , 36.37° , 44.35° and 54.07° are the main peaks observed in the diffraction analysis. The peaks at 25.29° and 44.35° correspond to hexagonal graphite lattice of the carbon spheres. The peak at $2\theta = 25.29^\circ$ with a broad diffraction signal from about 14° to 30° and an intensity of about 8800 (au) units indicates the presence of large amounts of amorphous carbon spheres in the as-prepared product.

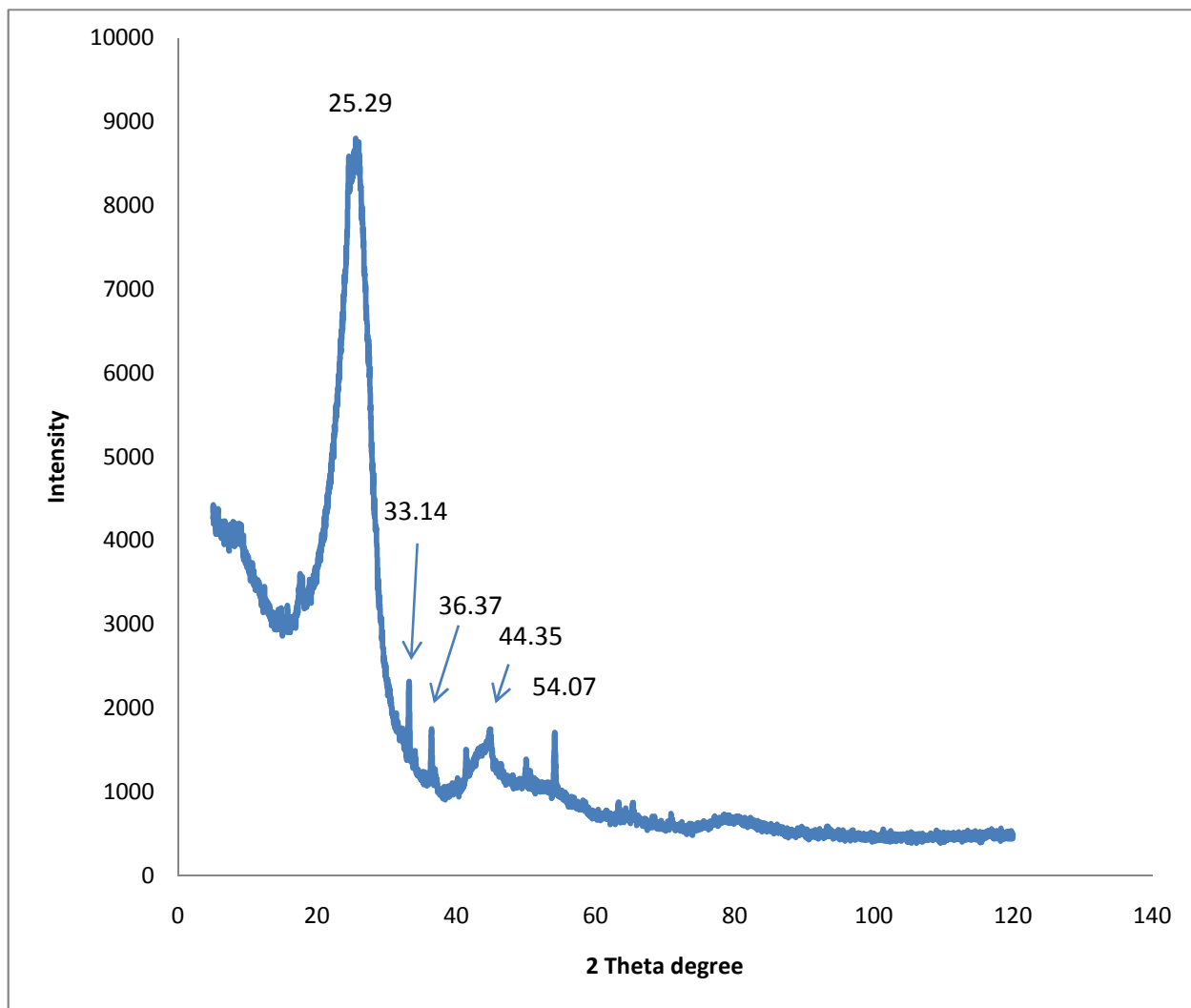


Figure 4.7: XRD pattern of carbon material as-prepared from bis(acetylacetonato)oxovanadium(IV)

There is a low intensity of the peak at $2\theta = 44.35^\circ$. The peaks at $2\theta = 33.14^\circ$, 36.37° and 54.07° correspond to crystal planes of (111), (200), and (220) of vanadium in the bis(acetylacetonato)oxovanadium(IV) catalyst precursor used in the synthesis.

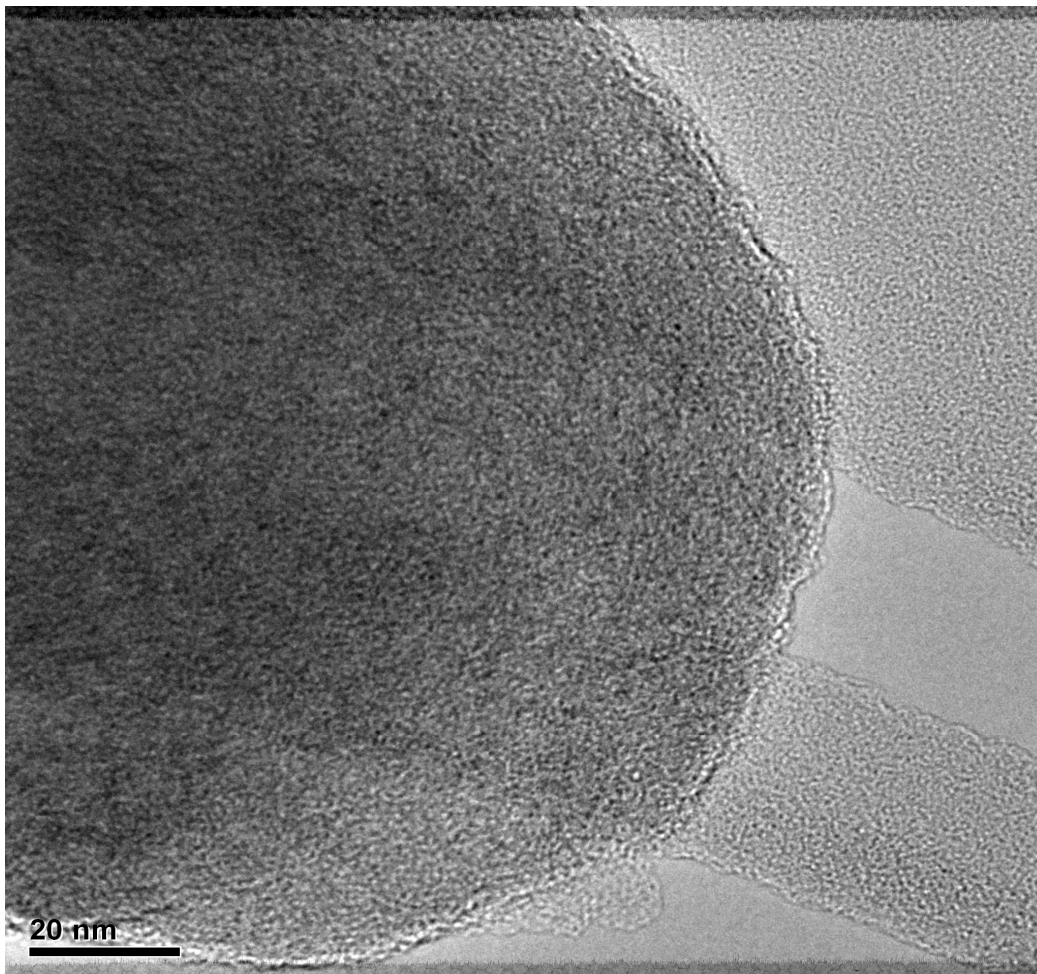


Figure 4.8(a): TEM micrograph of carbon material as-prepared from bis(acetylacetonato)oxovanadium (IV)

Transmission electron microscope (TEM) was used to measure the inner and outer diameter, assess structural integrity, and also to identify structural changes caused by surface modification. The TEM micrograph of the as-prepared carbon spheres is presented in Figure 4.8(a) and 4.8(b). Further morphological details of the spheres as observed in the SEM micrograph are corroborated in the TEM micrograph. The HR-TEM micrograph confirms the materials obtained in this synthesis as carbon spheres.

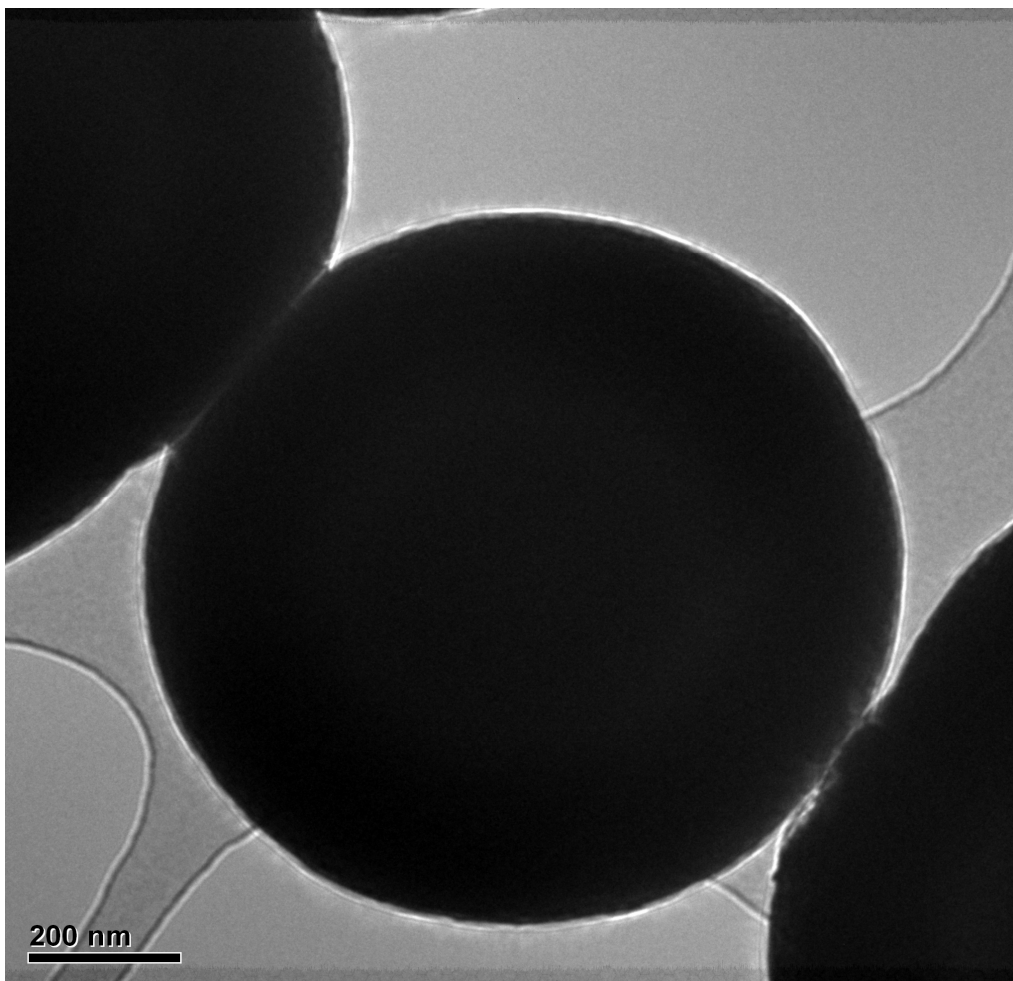


Figure 4.8(b): TEM micrograph of carbon material as-prepared from bis(acetylacetonato)oxovanadium (IV)

The TEM micrograph, Figure 4.8(a), show the morphology of a single carbon nanotube or several spheres that have encapsulated together. Figure 4.8 (b) is a magnified image of an individual sphere indicating the spheres to be uniform throughout with a diameter of about 87.5 μm .

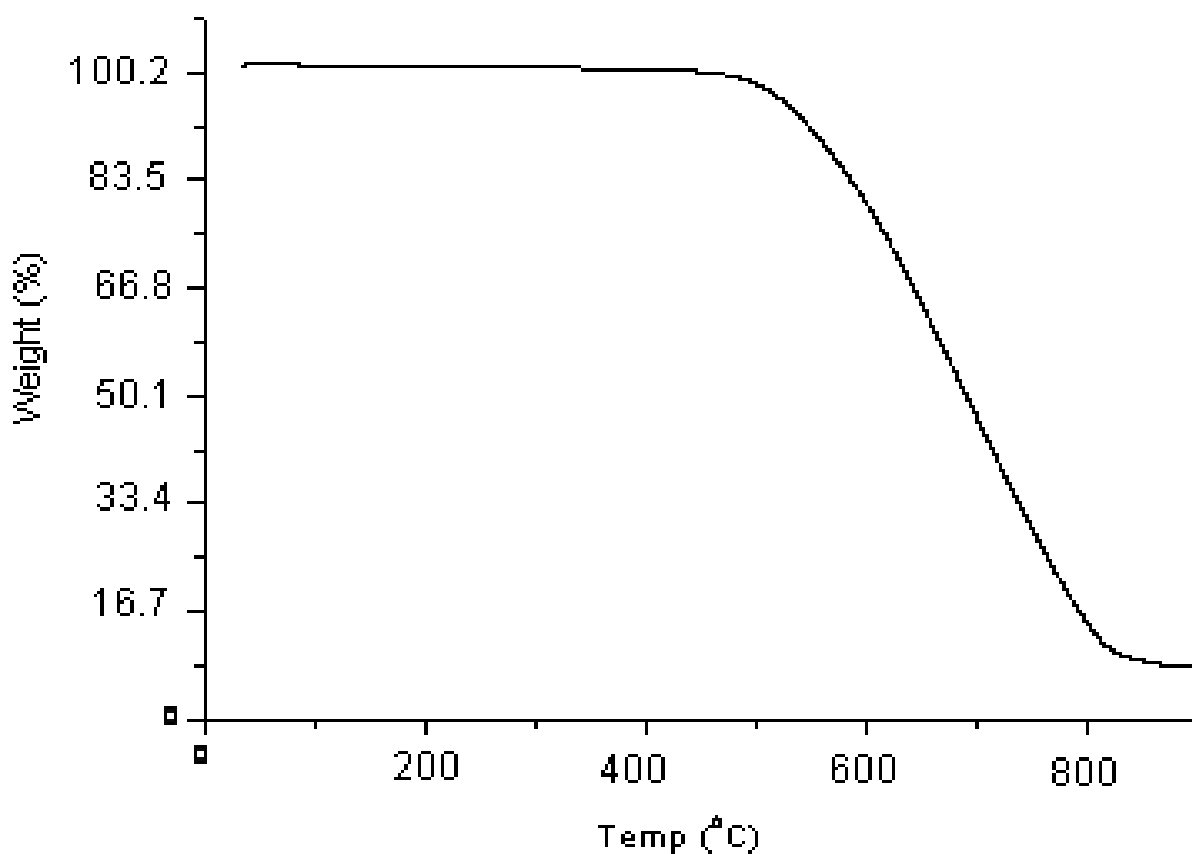


Figure 4.9: TGA graph of carbon material as-prepared from bis(acetylacetonato)oxovanadium(IV)

The thermogravimetric analysis (TGA) data of carbon spheres the as-prepared from bis(acetylacetonato)oxovanadium(IV) is presented in Figure 4.9. A uniform chemical reaction observed from 0°C to approximately 500°C is due to the amorphous carbon material burning. The weight loss from 500 °C to 700°C is that of the carbon spheres. The TGA data presented in Figure 4.9 presents approximately 92% weight loss. The remaining 8% is associated to the weight of the catalytic powder.

4.3.2 Carbon nanomaterial as-prepared from tris(acetylacetonato)oxomanganese (III)

The Raman spectrum of carbon material obtained from the as-prepared Manganese(III) acetylacetonate catalyst precursor is presented in Figure 4.10. Figure 4.10 shows two bands at 1338.16 and 1585.26 cm^{-1} which are D- and G- bands indicating the presence of crystalline graphitic carbon in a sample.

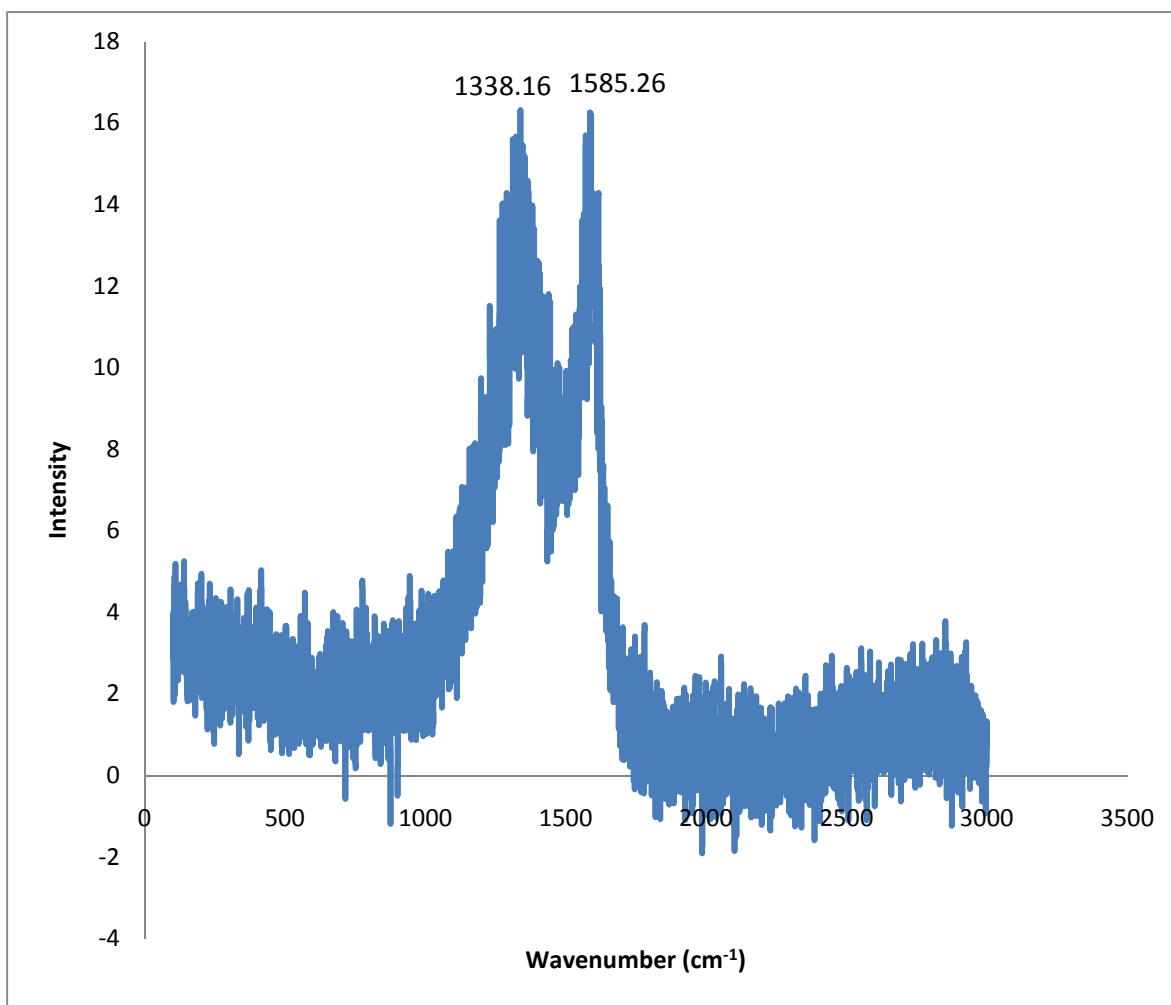


Figure 4.10: Raman spectrum of carbon material as-prepared from tris(acetylacetonato)oxomanganese (III)

The peak of the D-band appearing at 1338.38 cm^{-1} is due to the breathing modes of sp^2 atoms in the rings which arise due to the amorphous or non-crystalline carbon present in the material. The G-band observed at 1585.26 cm^{-1} corresponds to the splitting of E_{2g} stretching mode of graphite, which arises due to the tangential vibrations of the carbon atoms. The intensity ratio of the D- and G-bands (I_G/I_D) or the ration of their areas provides crucial information about the graphicity. The intensity ratio of the D- and G-bands (I_G/I_D) is 1.084.

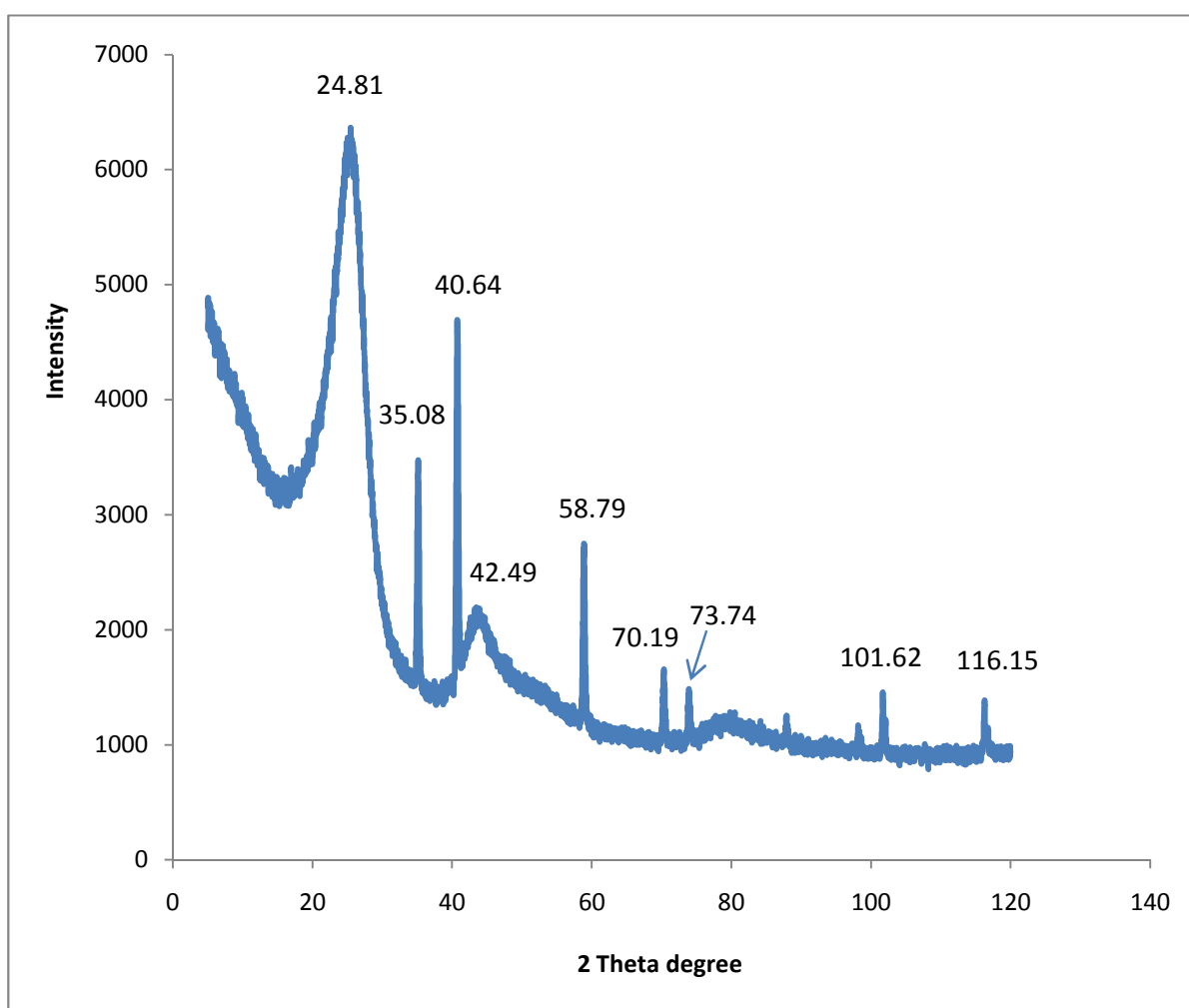


Figure 4.11: XRD pattern of carbon material as-prepared from Manganese(III) acetylacetonate

X-ray diffraction (XRD) pattern of carbon spheres obtained from the synthesized Manganese(III) acetylacetonate catalyst precursor is shown in Figure 4.11. Bragg diffraction peaks at $2\theta = 24.81^\circ$, 35.08° , 40.64° , 42.49° , 58.79° , 70.19° , 73.74° , 101.62° and 116.15° are the main peaks observed in the diffraction analysis. The peaks at 24.81° and 42.49° correspond to hexagonal graphite lattice of the carbon material. The peak at $2\theta = 24.81^\circ$ with a broad diffraction signal from about 20° to 34° and an intensity of about 6500 (au) units indicates the presence of large amounts of amorphous carbon material in the as-prepared product.

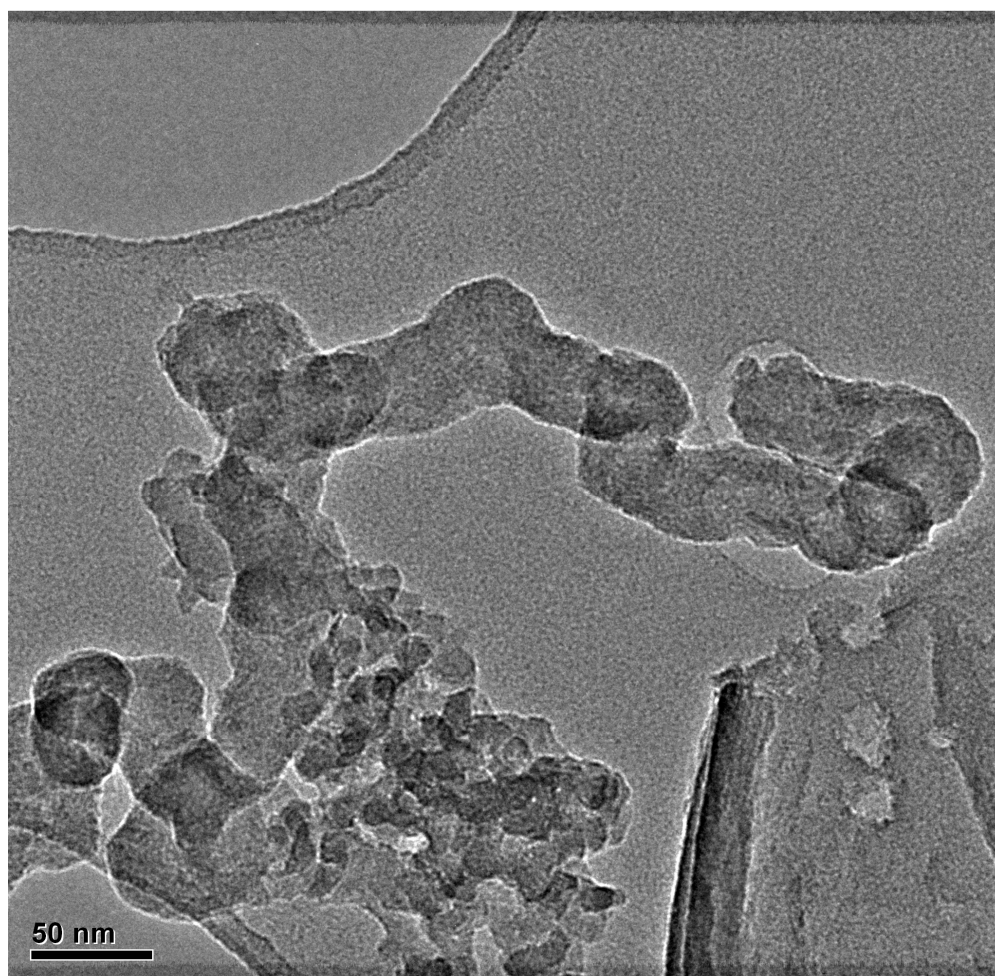


Figure 4.12(a): TEM micrograph of carbon material as-prepared Manganese(III) acetylacetonate

TEM micrograph in Figure 4.12(b) confirms the presence spheres in the sample. Several spheres have agglomerated together to form a chain with individual spheres seen to overlap together in Figure 4.12(a). The TEM micrograph, Figure 4.12(a), show the morphology of a single carbon nanotubes or several spheres that have encapsulated together. The TEM micrograph in Figure 4.12(b) is a magnified image of a single sphere indicating the presence of microspheres with a diameter of about 100 μm .

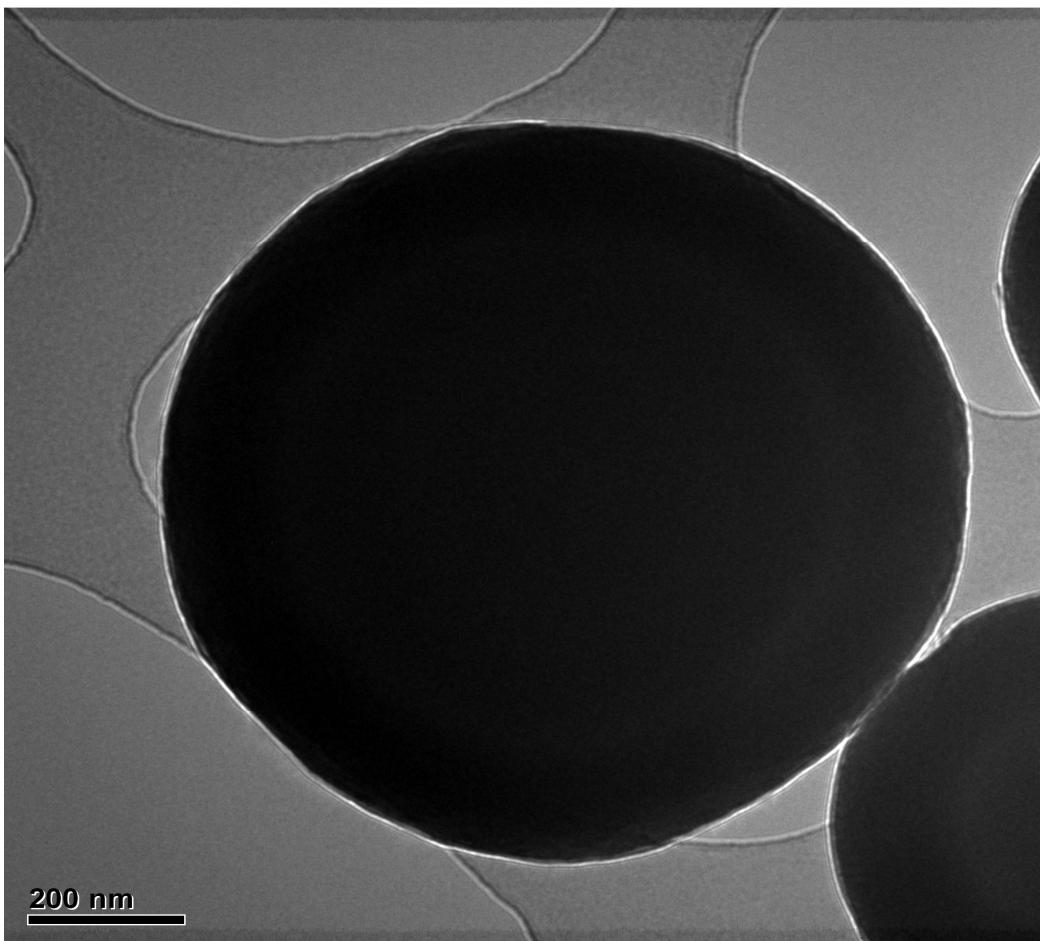


Figure 4.12(b): TEM micrograph of carbon material as-prepared Manganese(III) acetylacetonate

The interpretation of the TGA data is not often straight forward due to the composition of material and the weight of catalyst precursor that changes during the reaction. The TGA

data on Figure 4.13 shows a one step reaction that occurred during the chemical reaction.

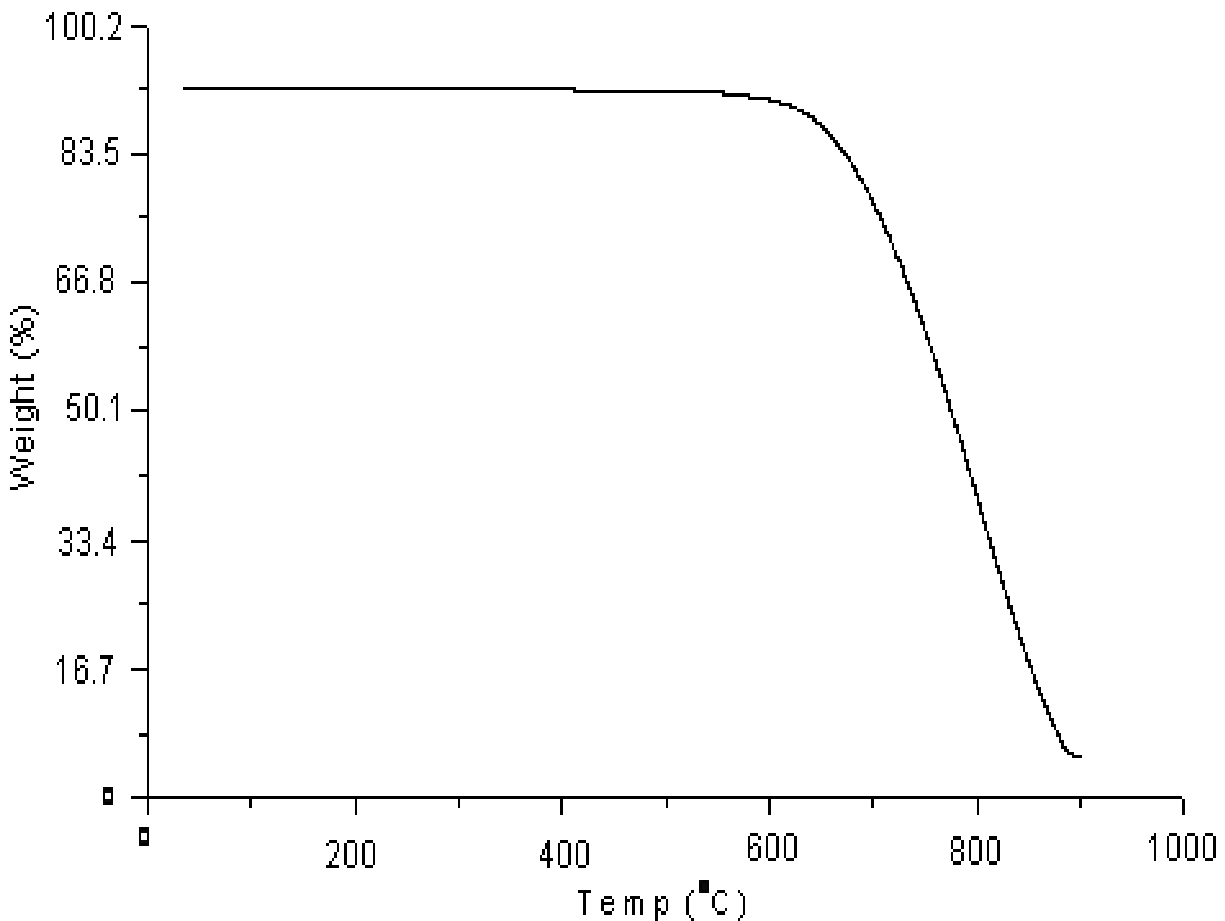


Figure 4.13: TGA data of carbon material as-prepared from Manganese(III) acetylacetonate

Figure 4.13 shows the TGA data of carbon material obtained from the as-prepared Manganese(III) acetylacetonate. The uniform chemical reaction observed from 0°C to approximately 600°C is due to the amorphous carbon material burning. The sample starts decomposing approximately at 600°C to 900°C. The TGA data presents approximately a 97% weight loss which is mainly attributed to a one step reaction process. The remaining 3% is associated to that of the catalytic powder. The thermal

stability observed in Figure 4.13 is an indication that the materials formed in the synthesis are carbon microspheres.

4.3.3 Carbon nanomaterial as-prepared from Co-Zn

The Raman spectrum of carbon material produced from synthesizing Co-Zn catalyst precursor is presented in Figure 4.14. Figure 4.14 shows, two major peaks: the D- and G-band. The D- and G-band are observed at 1299.38 and 1586.71 cm^{-1} respectively. The D-band at 1299.38 cm^{-1} is associated with the presence of amorphous carbon and non-crystalline carbon. The G-band at 1586.71 cm^{-1} indicates the presence of ordered materials. The intensity ratio of the D- and G-band (I_D/I_G) is 1.0904. The higher the intensity ratio, the higher the purity of carbon materials produced. A number of other peaks are observed at 666.73, 1122.25, 2112.63 and 3078.88 cm^{-1} . The peak at 1122.25 cm^{-1} is that of the T-band and is due to the amorphous carbon. The peaks appearing at 666.73 and 2112.63 cm^{-1} are due to the vibrations in the instrument while the sample is being characterized.

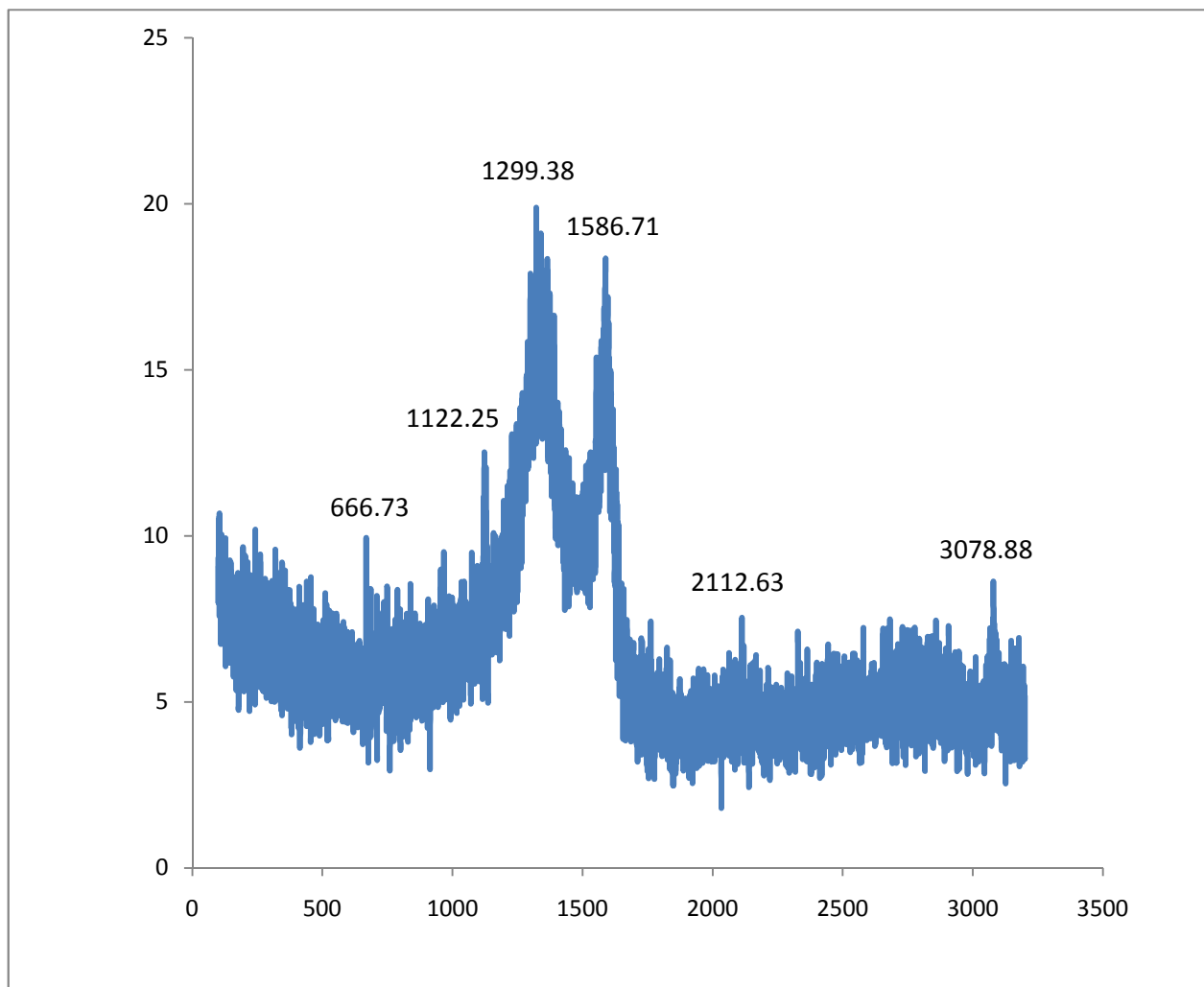


Figure 4.14: Raman spectrum of carbon nanomaterial as-prepared from Co-Zn

The particle shape and size were determined using the scanning electron microscopy (SEM). Figure 4.15 shows the presence of carbon nanotubes with traces of morphology or spherical particles that are attached to each other forming a chain-like structure that is observed in Figure 4.15. The fused spherical particles that are observed, can be associated to that of carbon nanospheres or morphologies of precursor's particles.

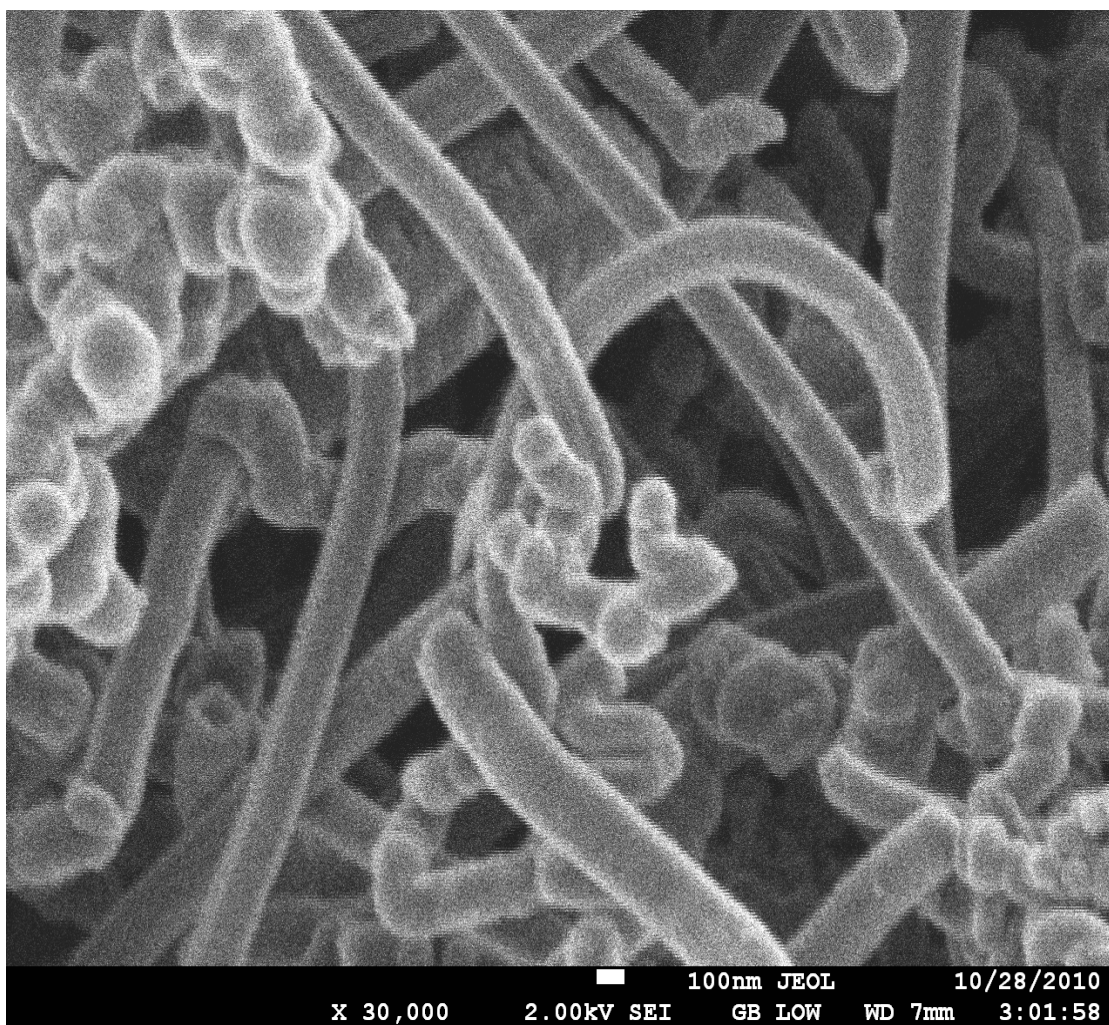


Figure 4.15: SEM image of carbon nanomaterial as-prepared from Co-Zn

Energy dispersive spectroscopy (EDS) spectrum of carbon nanotubes produced from the as-prepared Co-Zn catalyst precursor is presented in Figure 4.16. The spectrum shows the presence of carbon, oxygen, cobalt and zinc at 0.3, 0.5, 0.55 and 1.05 KeV respectively. Figure 4.16 indicates that the spectrum contains carbon as well as precursor's metals. The carbon is derived from the carbon nanotubes while cobalt and zinc are derived from the Co-Zn catalyst precursor.

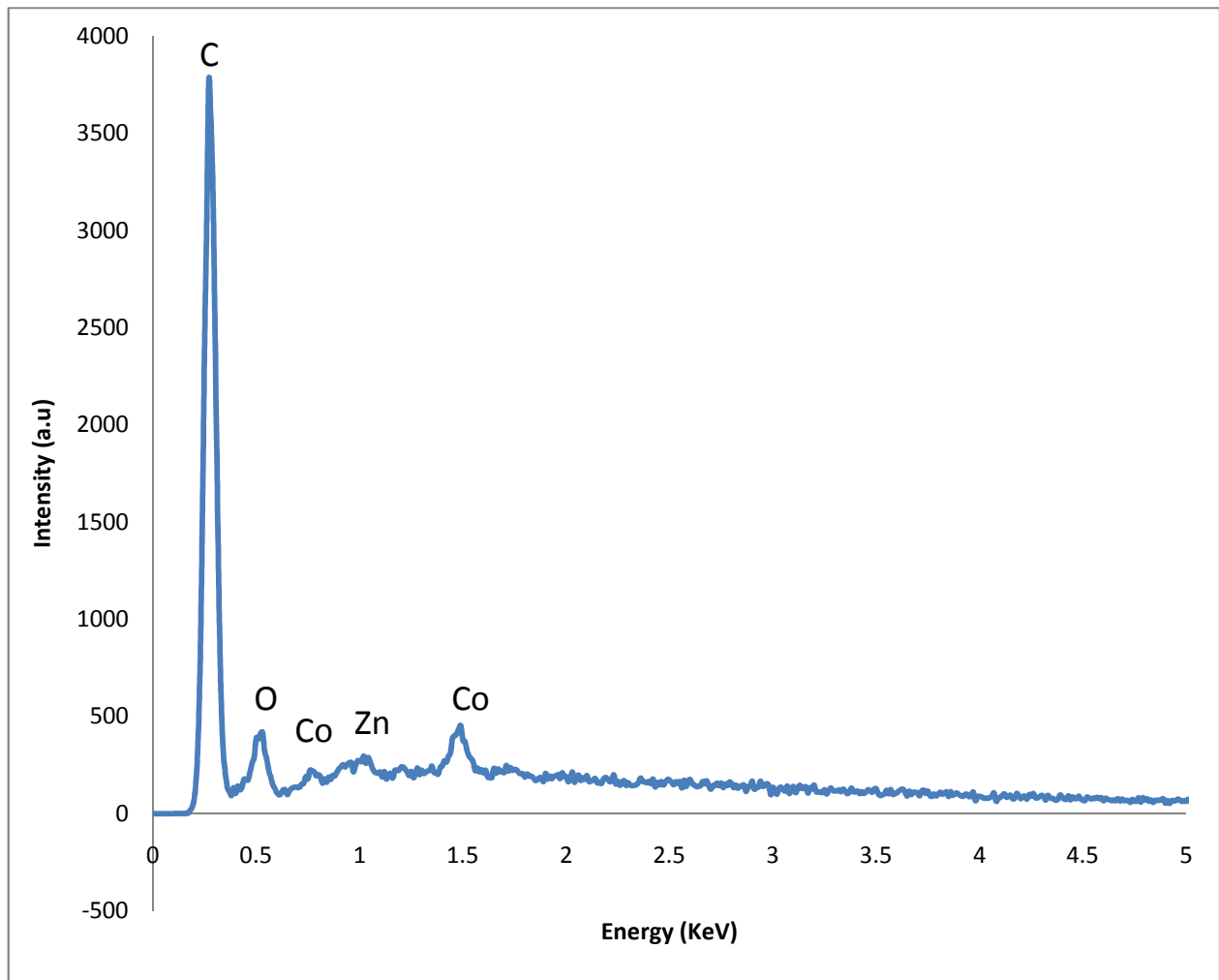


Figure 4.16: EDS spectrum of carbon nanomaterial as-prepared from Co-Zn

X-ray diffraction (XRD) pattern of the as-prepared carbon nanotubes is shown in Figure 4.17. Bragg diffraction peaks at $2\theta = 25.76^\circ$, 29.65° , 36.21° and 43.80° are the main peaks observed in the diffraction pattern. The peaks at 25.76° and 43.80° correspond to hexagonal graphite lattice of the carbon nanotubes.

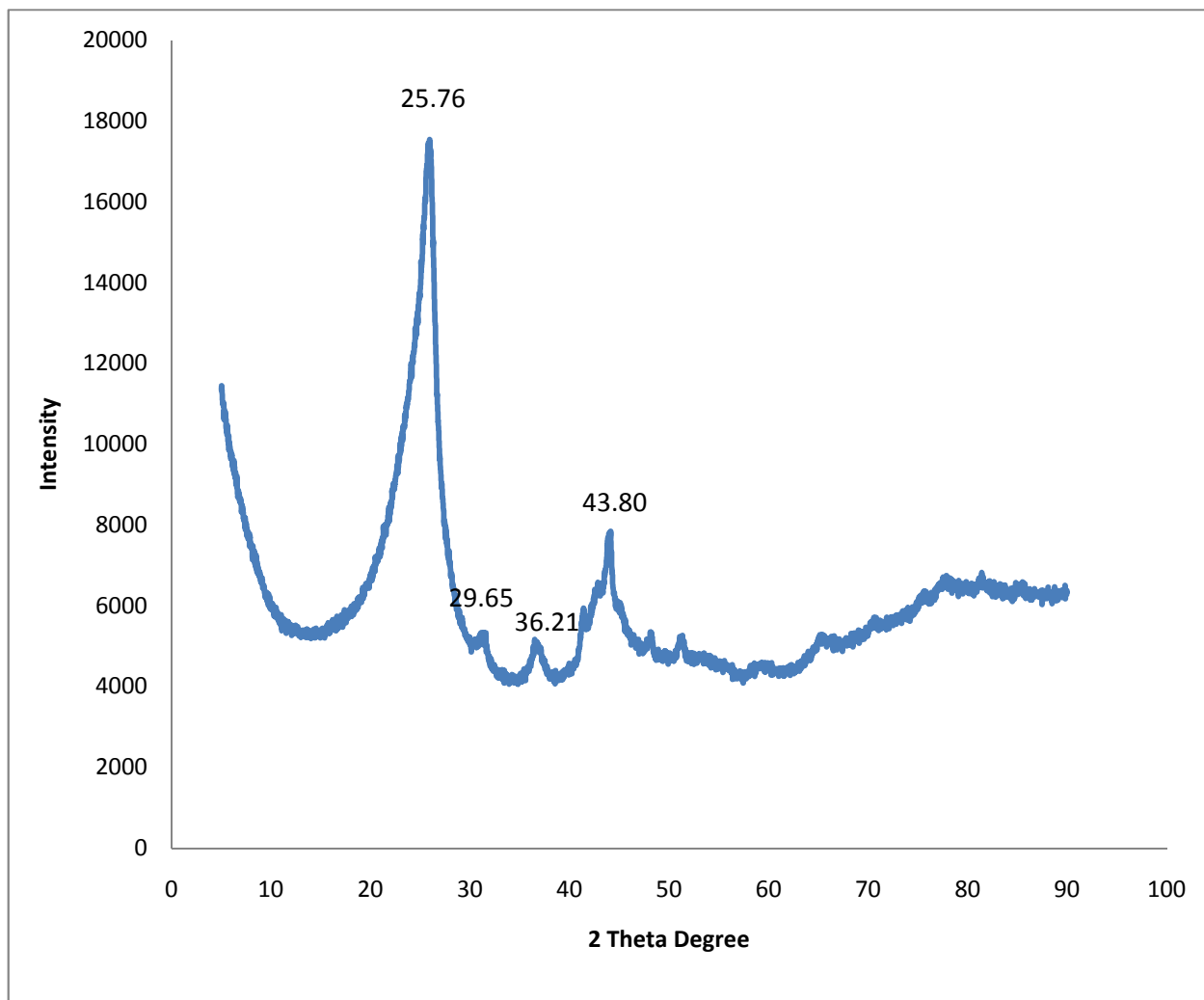


Figure 4.17: XRD pattern of carbon nanomaterial as-prepared from Co-Zn

The peak at $2\theta = 25.76^\circ$ with a broad diffraction signal from about 16° to 30° and an intensity of about 18000 (au) units indicates the presence of large amounts of carbon nanotubes in the as-prepared product. Figure 4.17 shows low intensity of the peak at $2\theta = 36.21^\circ$.

4.3.4 Carbon nanomaterials as-prepared from Co-Al

The Raman spectrum of carbon material consists of a graphitic or *G*-band, from highly ordered carbon material sidewalls, while disorder in the sidewall structure results in a *D*-band. In Figure 4.18 the *D*- and *G*-bands indicating the presence of crystalline graphitic carbon in carbon material are observed 1314.44 and 1591.26 cm^{-1} respectively. The *D*-band observed at 1314.44 cm^{-1} is due to the breathing modes of the sp^2 in the rings which arises due to the non-crystalline carbon present in the material where as the *G*-band appearing at 1591.29 cm^{-1} is that of ordered carbon material. The intensity ratio of the *D*- and *G*-bands (I_G/I_D) provides crucial information about the graphicity. The intensity ratio of the *D*- and *G*- bands (I_G/I_D) is 1.054. The overtone at 2483.21 cm^{-1} confirms that there is a carbon element in a sample.

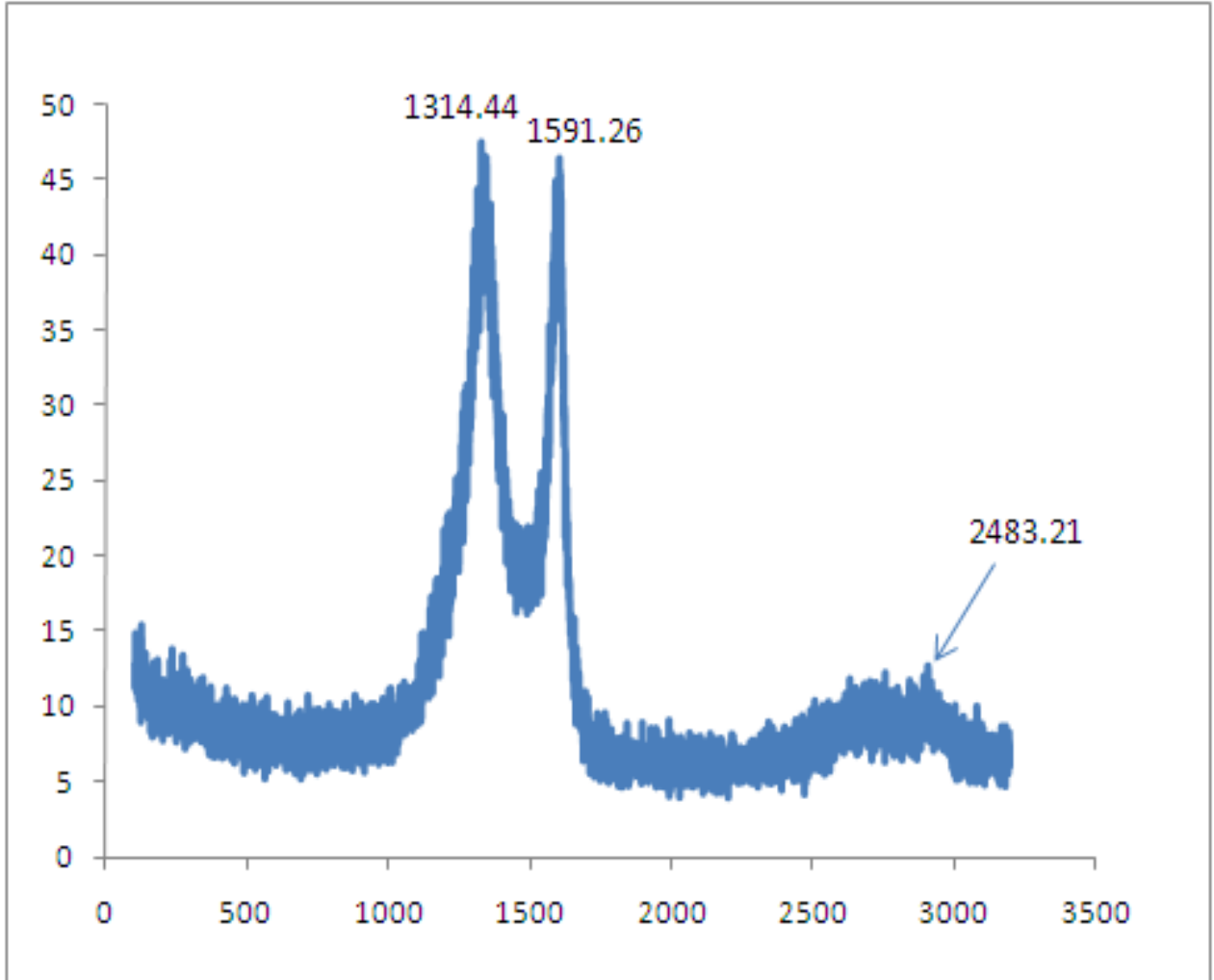


Figure 4.18: Raman spectrum of carbon nanomaterial as-prepared from Co-Al

The Scanning electron microscopy (SEM) image of carbon material obtained from the synthesized Co-Al catalyst precursor is presented in Figure 4.19. The SEM micrograph shows the presence of carbon nanotubes with traces of spherical particles. Figure 4.19 shows a very high purity of carbon nanotubes and because of the high magnification of the image, it is difficult to see properly the direction of growth of the nanotubes.



Figure 4.19: SEM image of carbon nanomaterial as-prepared from Co-Al

Energy dispersive spectrum (EDS) of material obtained from Co-Al catalyst precursor is presented in Figure 4.20. The spectrum shows the presence of carbon, cobalt and aluminium, cobalt and aluminium at 0.28, 0.73 and 1.35 KeV respectively.

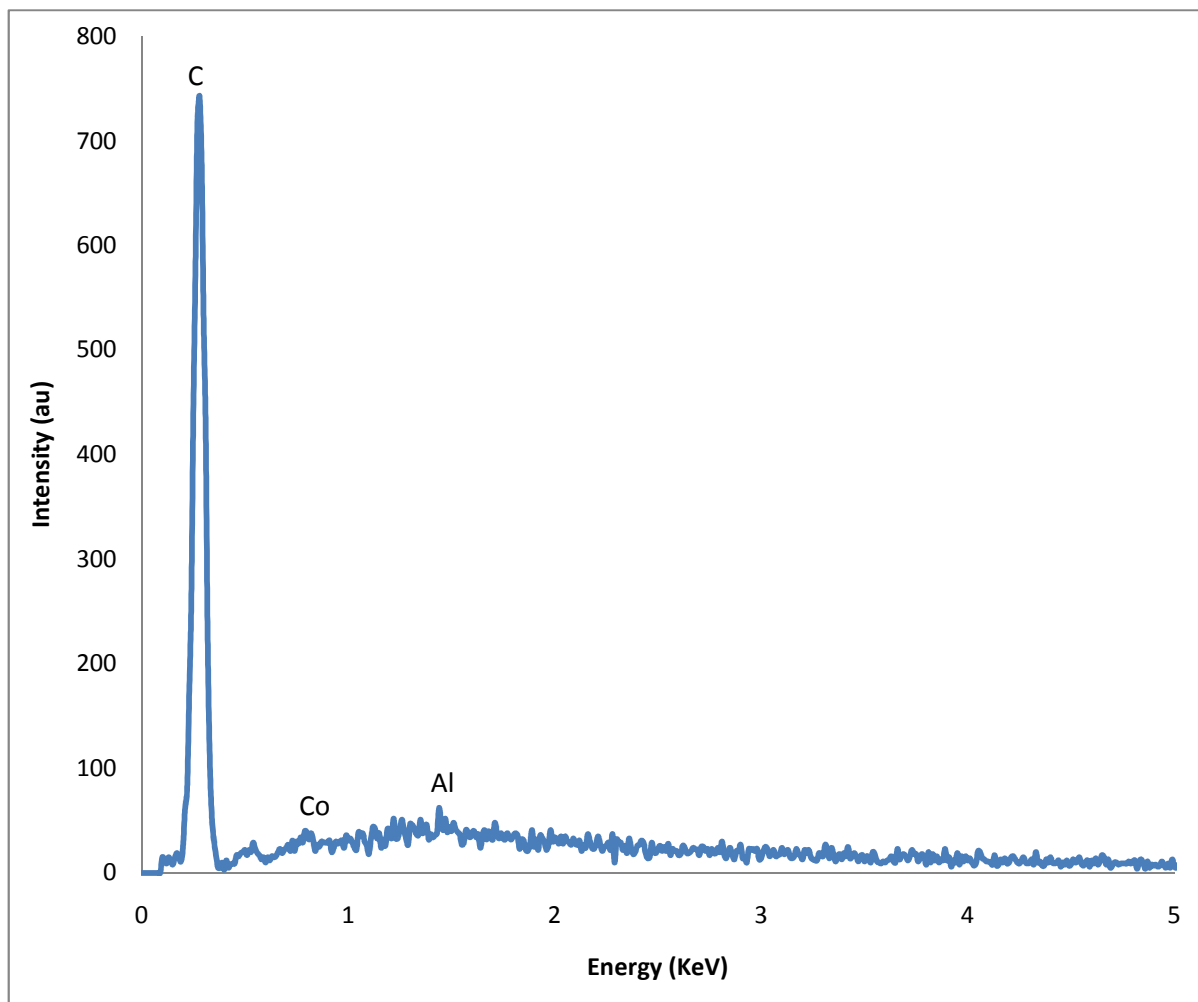


Figure 4.20: EDS spectrum of carbon nanomaterial as-prepared from Co-Al

Figure 4.20 shows the spectrum containing carbon as well as Cobalt and Aluminium metals. The carbon is derived from that of carbon nanotubes while cobalt and aluminium are derived from the catalyst precursor.

X-ray diffraction (XRD) pattern of the as-prepared carbon nanotubes from Co-Al catalyst precursor is presented in Figure 4.21. Bragg diffraction peaks at $2\theta = 25.79^\circ$, 31.83° , 36.18° , 41.48° and 43.93° are the main peaks observed in the diffraction analysis.

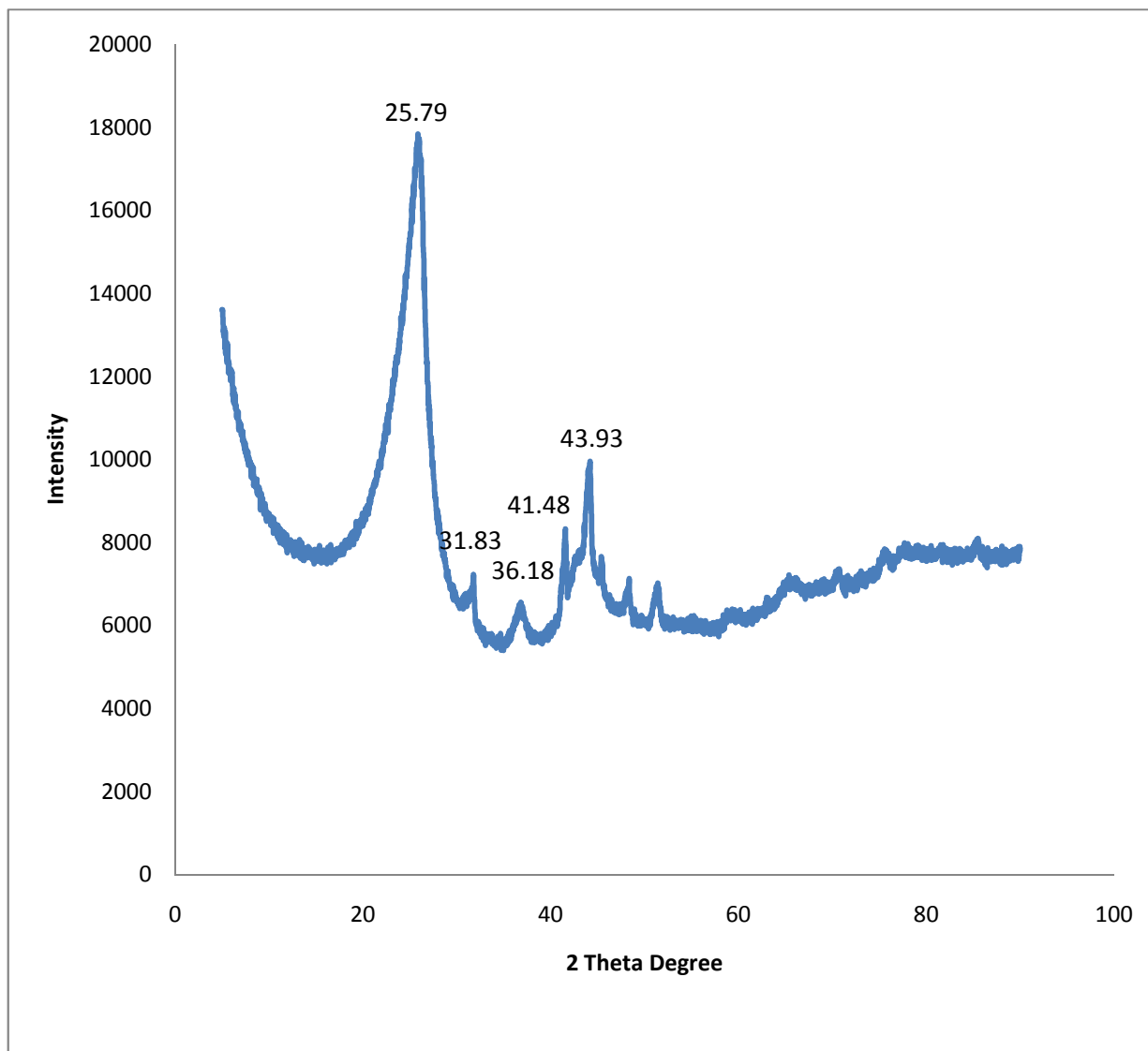


Figure 4.21: XRD pattern of carbon nanomaterial as-prepared from Co-Al

The peaks at 25.79° and 43.93° correspond to hexagonal graphite lattice of the carbon nanotubes. The peak at $2\theta = 25.79^{\circ}$ with a broad diffraction signal from about 18° to 30° and an intensity of about 18000 (au) units indicates the presence of large amounts of carbon nanotubes in the as-prepared product. The low intensity of the peak at $2\theta = 36.18^{\circ}$, is an indication of the quality of carbon nanotubes present in the as-prepared product.

5.1 CONCLUSIONS

The study drew a number of conclusions. The catalyst precursors bis(acetylacetonato)oxovanadium(IV) and Manganese(III) acetylacetonate were synthesized successfully using the catalytic chemical vapor deposition method to produce carbon materials in the presence of acetylene gas as carbon precursor. The SEM and TEM images proved that the carbon materials produced from the as-prepared catalyst precursors were carbon spheres of uniform diameter of 104 μ m and 87.5 μ m respectively. The Raman intensity ratio (I_G/I_D) for the synthesized bis(acetylacetonato)oxovanadium(IV) and Manganese(III) acetylacetonate catalyst precursors were proved to be 0.8556 and 1.084 respectively. Small amounts of amorphous carbon and a strand of carbon nanotubes were observed in the TEM micrographs. The TGA data shows the thermal stability of the as-prepared carbon nanospheres from both catalyst precursors when exposed to harsh conditions.

Co-Zn and Co-Al catalyst precursors were also successfully synthesized using the catalytic chemical vapor deposition method to produce carbon materials in the presence of acetylene gas as a carbon precursor. Carbon materials produced from synthesizing Co-Zn and Co-Al catalyst precursors indicates the presence of carbon nanotubes with small amounts of amorphous carbon present as observed in the SEM images. Synthesizing Co-Zn catalyst precursor yielded approximately 80% of carbon nanotubes, whereas synthesizing Co-Al catalyst precursor yielded approximately 98% of carbon

nanotubes. The thermal stability of as-prepared carbon nanotubes was determined by *Dikio et al. (2010)*.¹

This study therefore demonstrates the production of carbon spheres when synthesizing bis(acetylacetonato)oxovanadium(IV) and Manganese(III) acetylacetonate catalyst precursors, also demonstrates the production of carbon nanotubes when Co-Zn and Co-Al catalyst precursors has been synthesized. The XRD pattern identified the presence of amorphous carbon in the synthesis.

5.2 RECOMMENDATIONS

Carbon materials produced by the CCVD synthesis method contain traces of metal catalysts. The metal traces needs to be removed before nanomaterials are used for any industrial application.² One method used for their purification is through thermal oxidation in air prior to the removal of the metal catalyst by sonication in hydrochloric acid.³ Alternatively, the carbon materials can be heated under reflux in a sodium hydroxide solution for 2 days to remove the alumina support. Stirring in HCl for 5 hours removes the metal catalyst. These methods are harsh and do often introduce some functionality onto the carbon nanomaterials.⁴⁻⁶

REFERENCES

1. E.D. Dikio, F.T. Thema, C.W. Dikio, F.M. Mtunzi, *Int. J. Nanotech. Appl.* 4 (2) (2010) 117-124.
2. E.D. Dikio, N. Bixa, *Int. J. Appl. Chem.* 7 (1) (2011) 35-42.
3. B. Zhao, H. Hu, S. Niyogi, M.E. Itkis, M.A. Hamon, P. Bhowmik, M.S. Meier, R.C. Haddon, *J. Am. Chem. Soc.* 123 (2001) 11673.
4. R. Murphy, J.N. Coleman, M. Cadek, B. McCarthy, M. Bent, A. Drury, R.C. Barklie, W.J. Blau, *J. Phys. Chem. B.* 106 (2002) 3087.
5. T.W. Ebbesen, P.M. Ajayan, H. Hiura, K. Tanigaki, *Nature.* 358 (1994) 519.
6. V. Ivanov, A. Fonseca, J.B. Nagy, A. Lucas, P. Lambin, D. Bernaerts, X.B. Zhang, *Carbon.* 33 (1995) 1727.